CHALMERS

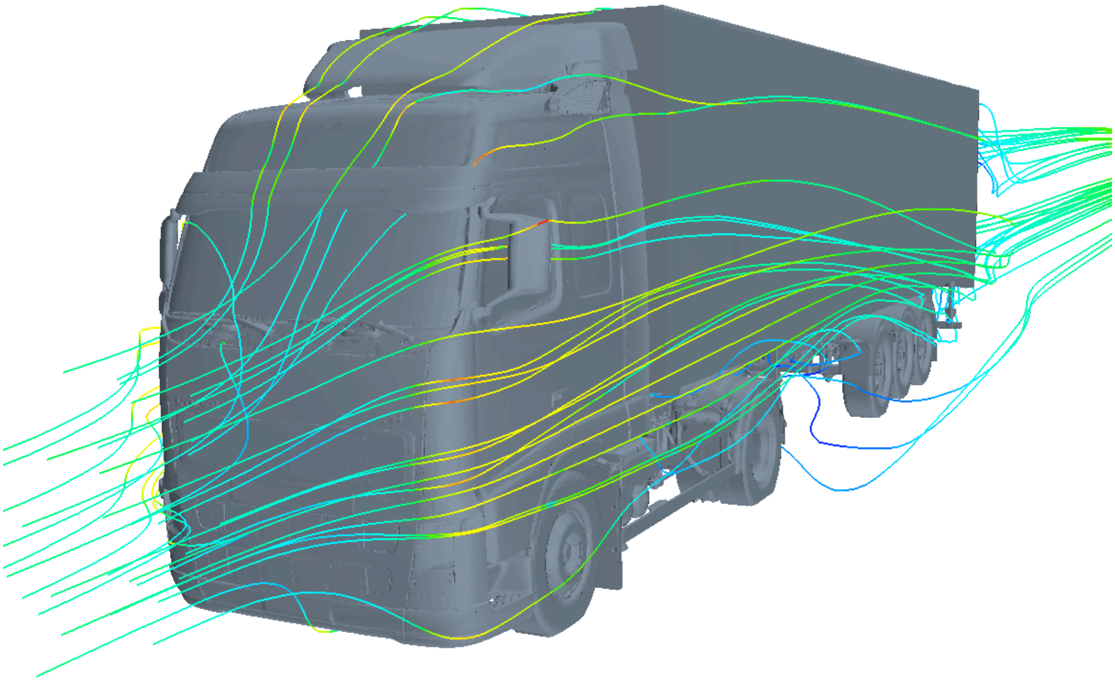

Aerodynamic Drag Reduction of a Heavy Truck with Variable Cooling Air Intake Area

Master's Thesis in the Master's programme Automotive Engineering

LISA LARSSON

HELENA MARTINI

Department of Applied Mechanics
Division of Vehicle Safety
CHALMERS UNIVERSITY OF TECHNOLOGY

Göteborg, Sweden 2009
Master's Thesis 2009:14

MASTER'S THESIS 2009:14

Aerodynamic Drag Reduction of a Heavy Truck with Variable Cooling Air Intake Area

Master's Thesis in the Master's programme Automotive Engineering

LISA LARSSON

HELENA MARTINI

Department of Applied Mechanics
Division of Vehicle Safety
CHALMERS UNIVERSITY OF TECHNOLOGY
Göteborg, Sweden 2009

Aerodynamic Drag Reduction of a Heavy Truck with Variable Cooling Air Intake Area
Master's Thesis in the Master's programme Automotive Engineering
LISA LARSSON
HELENA MARTINI

Master's Thesis 2009:14
ISSN 1652-8557
Department of Applied Mechanics
Division of Vehicle Safety
Chalmers University of Technology
SE-412 96 Göteborg
Sweden
Telephone: + 46 (0)31-772 1000

Cover:
Streamlines representing the velocity magnitude around a Volvo FH16 with a trailer.

Printed by Chalmers Reproservice
Göteborg, Sweden 2009

Aerodynamic Drag Reduction of a Heavy Truck with Variable Cooling Air Intake Area

Master's Thesis in the Master's programme Automotive Engineering

LISA LARSSON
HELENA MARTINI
Department of Applied Mechanics
Division of Vehicle Safety
Chalmers University of Technology

ABSTRACT

The extensive environmental debate of today forces vehicle manufacturers to develop new concepts with lower fuel consumption and emission levels than ever before. One way of reducing the fuel consumption is to improve the aerodynamic features of the vehicle. One source of drag is ascribed to the so-called cooling drag, which is defined as the resistance produced by the air passing through the underhood cooling system. A decreased amount of cooling air drag can result in substantial fuel consumption and emission reductions for heavy trucks.

The objectives in this research is to quantify the possible reduction in drag as a consequence of a restricted cooling air intake area for a Volvo FH16. Two approaches are used; the first method is to cover the grill area of the truck and the second method is to cover the cooling package. Two degrees of coverage exist in the study; the grill or the cooling system is either 100% covered or covered up to the Air Condition (AC) condenser. Another study that is carried out is to investigate the influence of a closed splitline.

The results are achieved by using Computational Fluid Dynamics (CFD) and the two commercial softwares ANSA and StarCCM+ are the tools used in this research.

The results from the simulations show that it is preferable to cover the grill compared to cover at the cooling package. Covering the grill and splitline of the Volvo FH16 results in a fuel consumption reduction of 2.3% compared to the original truck configuration. A trend that is clearly seen is that a closed splitline always decreases drag for all the tested truck configurations.

Even though a closed grill is preferred compared to a closed cooling package, it can still be worth to develop a technical solution for covering the cooling package if no suitable technical solution can be found for covering the grill. The reduction in drag for a covered cooling package is still quite substantial. The case with fully covered cooling package shows a fuel consumption reduction of 1.2%. As a conclusion it can be said that restricting the cooling air intake area for the Volvo FH16 can result in a substantial fuel consumption reduction.

Key words: drag reduction, cooling system, truck, aerodynamics, CFD

Contents

Nomenclature

A_f	Vehicle frontal area $\left[m^2\right]$
C_d	Drag coefficient [-]
$\Delta C_{d,\%}$	Percentage change in C_d between two cases [%]
$FC_{red,\%}$	Fuel consumption reduction between two cases [%]
F_d	Drag force [N]
$\dot{m}_X$	Mass flow of air through cooling system component X $\left[\frac{m^3}{s}\right]$
p	Static pressure [Pa]
P	Power [W]
ρ	Air density $\left[\frac{kg}{m^3}\right]$
V	Vehicle velocity $\left[\frac{m}{s}\right]$
V_a	Air velocity $\left[\frac{m}{s}\right]$
V_r	Vehicle velocity relative to the air $\left[\frac{m}{s}\right]$
$y+$	Dimensionless wall distance [-]

Abbreviations

AC	Air Condition
CAC	Charge Air Cooler
CAD	Computer Aided Design
CFD	Computational Fluid Dynamics
DC	Drag Counts
FC	Fuel Consumption
FE	Finite Element
PID	Property Identification
RANS	Reynolds-Averaged Navier-Stokes
UTM	Underhood Thermal Management

Acknowledgment

The authors of this master thesis work, Lisa Larsson and Helena Martini, would like to acknowledge some persons that have guided us through this project.

Firstly, we would like to thank Volvo 3P for giving us the opportunity to implement such an interesting thesis work. During this period we have had a lot of support and guidance from the employees at the company. We would like to thank Erik Dahl, our thesis supervisor at Volvo 3P. We would also like to give a special thank to Torbjörn Wiklund who has been our main software support during this period. Furthermore, many thanks to Zenita Chronéer, Linus Hjelm and Benjamin Olaisson for given us necessary information for the procedure of our work.

Secondly, we would like to acknowledge a few persons at Chalmers University of Technology. A great thank to our excellent supervisor Licentiate Peter Gullberg, who has supported and guided us through this thesis work. We would also like to thank our examiner Professor Lennart Löfdahl for giving us the opportunity to develop our skills in the field of aerodynamics and for having trust in us. Also, a special thank to Licentiate David Söderblom and Licentiate Christoffer Landström for the help and support during the project.

Finally, we would like to thank our families and friends for their support and for showing interest in our thesis work.

1 Introduction

One of the most important and challenging issues in the vehicle industry today is to develop vehicles with as low fuel consumption as possible. This major objective descends from the heavy environmental debate which forces the vehicle companies to improve and renew their concepts.

There exist many different approaches for decreasing the fuel consumption; one of them is to decrease the aerodynamic resistance of the vehicle. The focus in this research will therefore be to reduce the aerodynamic resistance by changing the size and construction of the air intake area to the underhood cooling system for a given truck model. This new concept is intended to change the size of the cooling air intake area depending on the cooling performance required by the vehicle. The aerodynamic resistance for the different designs is calculated by running simulations using commercial Computational Fluid Dynamics (CFD) softwares.

Nowadays, CFD is a well recognized tool in the automotive industry for designing the vehicles of the next generation. CFD can be applied to a wide variety of topics within the field of road vehicle aerodynamics such as external and internal aerodynamics, but as well Underhood Thermal Management (UTM). This research deals both with aspects of UTM and external aerodynamics.

1.1 Background

Nowadays, new legislations regarding emission levels for vehicles are developed constantly. The permitted levels of these quantities are becoming more and more limited. This forces the vehicle manufacturers even more to develop vehicles that are within the permitted limits regarding emissions. Therefore, the companies have to find different areas where the vehicle can be improved in a way that the fuel consumption and hence the emissions are reduced. All vehicles operating at some speed above $0\,km/h$ are subjected to a resistance force commonly known as the aerodynamic drag. By reducing this resistance the fuel consumption will be decreased. A part of the aerodynamic drag is ascribed to the cooling air drag, which is the resistance produced by the air passing through the underhood cooling system. This system includes three parts, the Air Condition (AC) condenser, the Charge Air Cooler (CAC) and the radiator. Hence, one way to reduce the fuel consumption is by investigating the reduction of aerodynamic drag as a function of cooling air intake area.

The resistance that arises in the cooling system is partly due to the viscous dissipation in the cooling system, but as well due to the detrimental effects of the cooling airflow on external aerodynamics. The airflow through the cooling system serves mainly three purposes, the first is to keep down the temperature of the combustion engine, the second is to lower the intake air temperature to the turbocharger and the last purpose is to change the temperature in the vehicle compartment. Though, most truck cooling systems of today are over dimensioned for common vehicle usage, for example highway driving. They are dimensioned towards critical operating conditions, such as hot-day hill climbs.

This will e.g. result in a greater cooling potential than needed for cold climate cruising conditions. Hence for these conditions the vehicle will operate with higher drag, as compared to if the cooling system was dimensioned for cruise conditions. If the cooling airflow through the grill and the cooling system could be decreased, the cooling air drag would decrease and thereby also the fuel consumption. A possible way of reducing the cooling drag can be to apply variable cooling air intake areas, which are changing size depending on the driving conditions. A positive side effect of the decreased cooling air drag is that the engine will experience a shorter warm-up time if the air flow through the cooling system is limited, which is good from a fuel economy point of view as well. There may be other advantages when decreasing the intake area to the underhood, such as less dirt on the cooling package and less noise will be experienced.

BMW is one of the companies that have used this technique to decrease the vehicle resistance. They have invented a system for varying the cooling air intake area and it thereby controls the amount of cooling air entering the underhood area for a passenger vehicle. The system is called Air Vent Control and by using this system the total air resistance and hence the fuel consumption is lowered. On the BMW website [1] the following can be read about the Air Vent Control.

"A constant airflow through the radiator increases air resistance and affects aerodynamics. Electrically controlled vents in front of the radiator open and close the cooling air inlets so that the vents are only opened if cooling air is required. When the vents are closed, air resistance is reduced, as is fuel consumption."

There are other vehicle manufacturers that have made efforts in finding similar ways to control the cooling air flow. Any similar concept has not yet been developed by Volvo AB, but in this research the potential of such a system should be quantified.

1.2 Objectives

The objective in the research is to quantify the possible reduction in aerodynamic drag obtained by changing the design of the air intakes to the cooling system of a heavy truck, in this case a Volvo FH16. The drag reduction is quantified by using commercial CFD softwares. In more detail, the properties that are analyzed are the total drag change for the vehicle as well as the mass flow of air through the AC condenser, the CAC and the radiator. This investigation will consider the above presented parameters when the vehicle is simulated to drive in 90 km/h.

1.3 Delimitations

The analysis only includes the subjects mentioned in the objectives, including different designs of the air intake to the cooling system, the relative reduction in drag and the mass flow of air through the cooling system. Among with this limitation, there are a few other aspects that will not be included.

- The study is based only on the presented truck and trailer configuration described in Chapter 3.
- The model used will not include any heat exchange between the different parts in the cooling system.
- The fan is not rotating in the simulations.
- Any sources of noise related to the restricted air intakes to the cooling system will not be considered.
- There will not be any study of a possible unfavorable dirt distribution as a consequence of the changed design of the cooling air intakes.
- A development of a technical solution for solving the variable cooling air intake area is not included.
- The results will only be related to CFD simulations, no wind tunnel experiments or on road tests will be performed.
- The research is not intended to be a study of the drag in the sense that the results should be comparable to other trucks. The drag results should only be seen as change in drag and function as an indication of how much the drag can be lowered with a variable cooling air intake area.

1.4 Methodology

CFD is used in order to receive the results from the simulations and to be able to characterize the flow around the vehicle. Two CFD softwares are used in this research to obtain the results; these are ANSA and StarCCM+. Each program represents different operations in the CFD process, which can be divided into five steps. These can be denoted and described as follows.

1. CAD Cleaning
   The Computer Aided Design (CAD) cleaning process is the first step. At this stage, the CAD geometry is cleaned up from unwanted details which are not necessarily needed in order to receive accurate results. It is also possible to make larger geometry changes; parts can be removed or added if desired. It is of great importance that the geometry is cleaned up from e.g. sharp edges and holes so the software can solve the airflow around these parts.

2. Surface meshing
   The second step is the surface mesh generation, which together with the CAD cleaning is the most time consuming step in the process. At this stage, a mesh is created at the surface of the object. The surface mesh is generated in order for the volume mesh to have something to attach to. This mesh can be generated in two ways; by adding a surface mesh and by wrapping the model. The difference between these two operations is that a surface mesh will just add a mesh to the existing surface while a wrapped surface also closes small holes. When the surface mesh is created the model consists of a number of surface cells. Figure 1 shows a surface meshed truck and trailer model.

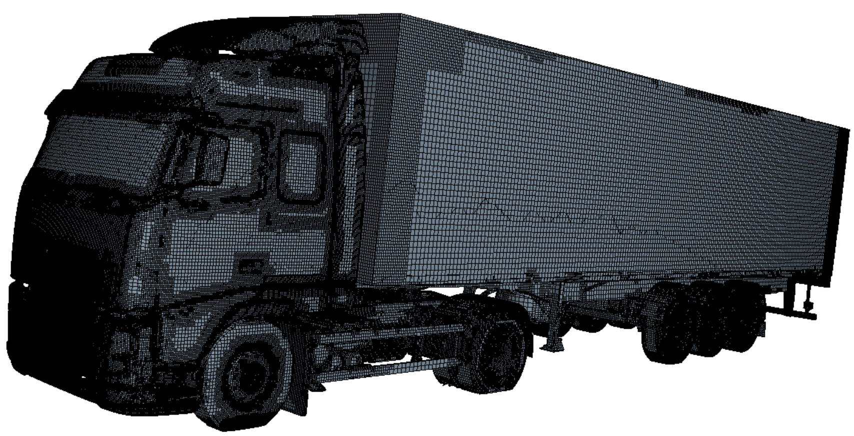

Figure 1: Surface mesh on a truck and trailer model

3. Volume meshing
   The third step is to generate a volume mesh. The software creates a number of three dimensional cells based on settings done by the user. The defined equations for the case will be solved in each cell. In general, a larger amount of cells yields a more accurate and reliable solution. To be able to add a volume mesh there must be boundaries around the model which correspond to the wind tunnel walls limiting the volume mesh. Figure 2 shows a plane which visualizes the volume mesh.

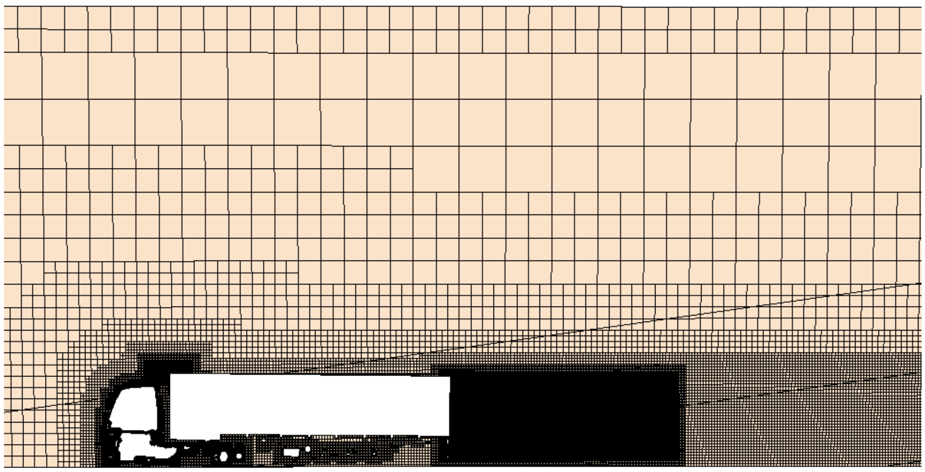

Figure 2: Volume mesh around a truck and trailer model

4. Solver
   During the fourth step, the pre-defined equations is solved iteratively in each of the volume cells. This is performed until convergence is reached, which is when the residuals of all variables remain at an approximately constant level from iteration to iteration.

5. Post-processing
   The fifth step represents the post-processing of the simulation. In this step the results from the simulation are visualized, for example by extracting numerical results and plots. Figures of the flow field around the object, showing properties which are relevant for the study, can also be generated.

The software ANSA is used for the CAD cleaning process while StarCCM+ is used for the remaining four steps. ANSA can be seen as the tool which makes it possible to go from CAD or Finite Element (FE) model to CFD solver.

StarCCM+ solves the predefined equations and calculates the flow in each volume cell iteratively to reach a solution according to the settings done by the user.

2 Theory and previous research

To understand the behavior of the flow field around a vehicle some basic aerodynamic theory is presented in this chapter. There has been a quite substantial amount of previous research in the area of cooling air drag and what reductions that can be achieved with a covered cooling system. It is known that the cooling air drag for a truck comprises about 2.5% of the total aerodynamic drag, while the corresponding value for a passenger car is $10-20\%$. Even though the percentage of cooling drag for a truck is not as high as for a passenger car, it is still important to improve this source of resistance since the possible amount of fuel savings for a truck could be of considerable importance.

2.1 Aerodynamic resistance

The aerodynamic resistance in terms of cooling air drag is an important aspect to analyze. On one hand it is of great importance that there is enough cooling to prevent an overheated engine but on the other hand it may be desirable to reduce drag to improve fuel economy. According to Ding, Williams and Karanth, a higher engine power requires higher amount of airflow through the underhood for engine cooling. Though, when more cooling is needed there is an advantage to have a greater air intake area to get sufficient air cooling [4]. Research carried out by Kuthada and Wiedemann [6], shows that there will be a change of the aerodynamic properties in terms of increased resistance of the vehicle when adding airflow through the underhood. This change is commonly referred to as the cooling air drag and is defined as the difference between the measured drag of the vehicle with cooling airflow and the drag of the same vehicle without any air cooling.

The aerodynamic resistance is provided by a factor called the drag coefficient, C_d, which corresponds to the entire aerodynamic resistance for the vehicle. This factor is mainly dependent on the shape of the vehicle. The research made by Kuthada et al [6] shows that the cooling drag coefficient is increased for vehicles with air cooling compared to vehicles without air cooling. Therefore, the airflow through the underhood should be kept as small as possible, but it should still satisfy the engine cooling and the climate control. Barnard [3] states that aerodynamic drag is partly produced due to the pressure distribution around the vehicle and partly due to the viscous dissipation which occurs due to the frictional or shearing action of the flow over the surface.

When changing the design of the air intake area the pressure around the vehicle will be affected. Barnard [3] states that it is desirable to have as low pressure difference between front and rear of the model as possible, since it will generate less pressure drag and hence result in a lower C_d value. The flow around the vehicle reaches the highest pressure just before entering the underhood, while the pressure is lower at the airflow exit. The lower the pressure at the exit, the more air flows through the CAC, the radiator and the AC condenser, according to [4]. Söderblom [7] further states that the major contribution to the total aerodynamic drag for heavy trucks is the drag produced by the pressure difference between the front and rear of the vehicle.

Jama, Watkins and Dixon [5] found from wind tunnel tests that sealing the entire front of a Ford Falcon, a modern passenger car, resulted in a drag reduction of 7%. From the results it is also seen that the drag coefficient is decreasing almost linearly with increased fraction of covered air intake.

2.2 Drag force and Power

Barnard states that the drag force, F_d, is one of the most important aerodynamic factors. This is a measure of the entire vehicle aerodynamic resistance for forward motion. The expression of the drag force is defined in Equation 1 , where ρ is the density of the surrounding medium, A_f is the frontal area of the vehicle and V_r is the vehicle velocity relative to the air [3].

$$F_d = \frac{1}{2} C_d \rho A_f V_r^2 \tag{1}$$

Hence, the drag force increases with the square of the velocity and is proportional to the C_d value.

The needed power to overcome the drag force is calculated by multiplying the drag force with the vehicle velocity. The expression is seen in Equation 2.

$$P = F_d V \tag{2}$$

When a vehicle is driving on a road it is exposed for both drag resistance and rolling resistance. Figure 3 presents a graph which shows the relation between these two resistances, the required power and the vehicle speed for a heavy truck.

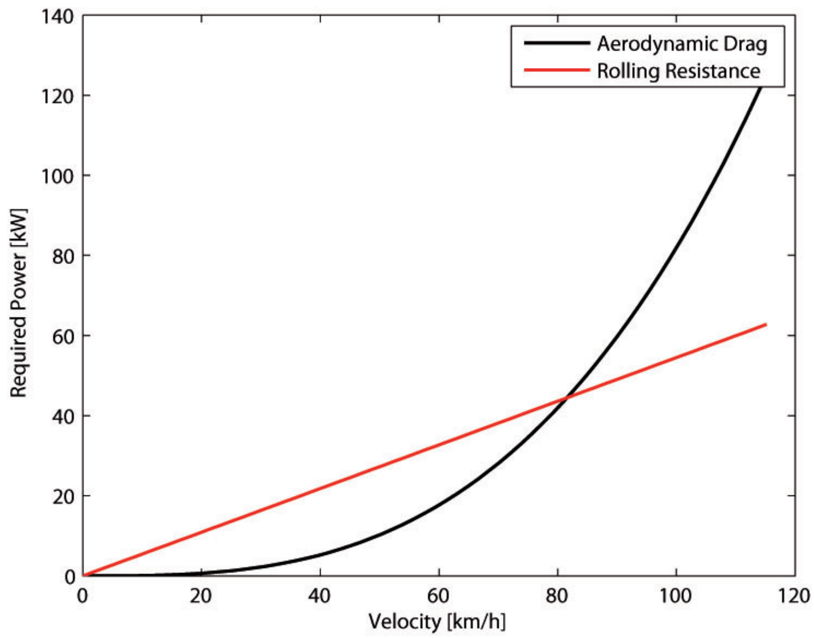

Figure 3: Required power for drag and rolling resistance as a function of vehicle velocity [7]

It is clearly seen that the aerodynamic drag is dominating at speeds above $80km/h$. This critical speed is valid for heavy trucks [7].

2.3 Bernoulli equation

The Bernoulli equation is fundamental to the study of the airflows around a vehicle according to Barnard [3]. This equation gives a relationship between the air speed and pressure at a specific area. For an aerodynamic analysis it is preferable to write this equation on the form presented in Equation 3, where p is the static pressure, ρ is the density of the air and V is the air speed.

$$p + \frac{1}{2}\rho V_a^2 = constant \tag{3}$$

Since the sum of the two terms is constant it follows that; an increase in pressure must generate in a decrease in the air velocity at the same spot. This makes it possible to only investigate the velocity distribution figures for a vehicle and from there knowing that the pressure distribution is the opposite due to the Bernoulli equation, or vice versa.

2.4 Drag reduction

One way of comparing the aerodynamic resistance is by analyzing the change in drag counts (DC) for different vehicle designs. These values are given by comparing the C_d values for one case in relation to a reference case. The expression for calculating the drag counts difference between two cases is shown in Equation 4, where DC_{change} is the drag count change.

$$DC_{change} = (C_{d,CaseX} - C_{d,ref}) \cdot 1000 \tag{4}$$

The percentage change of C_d between two cases can be expressed as $\Delta C_{d,\%}$ which is defined in Equation 5. This parameter is another way of comparing the aerodynamic drag for different case set-ups.

$$\Delta C_{d,\%} = \frac{(C_{d,CaseX} - C_{d,ref})}{C_{d,ref}} \cdot 100 \tag{5}$$

2.5 Fuel consumption

As a consequence of reduced aerodynamic drag the fuel consumption will be decreased. According to Söderblom [7] the reduction in fuel consumption compared to a reference case makes one third of the percentage reduction of aerodynamic drag. The relationship between reduction in drag coefficient and fuel consumption reduction is shown in Equation 6, where $FC_{red,\%}$ is the fuel consumption reduction in percent.

$$FC_{red,\%} = \Delta C_{d,\%} \cdot \frac{1}{3} \tag{6}$$

2.6 Mass flow of air

To get an impression of the cooling performance of the cooling system the amount of air which passes through the AC condenser, the CAC and the radiator can be measured. Comparing the mass flow of air through each part of the cooling system for different vehicle designs provides an indication of how much air that passes through the system compared to the measured drag coefficient. Analyzing the mass flow of air passing the cooling system makes it quite straightforward to decide which vehicle design that has the most suitable combination of airflow through the cooling system and aerodynamic resistance.

3 Case definitions

The vehicle that is used for simulations is a Volvo FH16 with a 12 meter long trailer. This is a heavy truck from the Swedish brand Volvo, with a 16 liter diesel engine. The length of the entire truck and trailer is close to 15 meters. The height of the equipage is 4.1 meters and the truck has a frontal area of $10.64\,m^2$. The vehicle is shown in Figure 4.

Figure 4: Volvo FH16

As can be seen in Figure 4, there are a few drag reducing devices mounted on the truck. There is an air deflector which guides the airflow from the truck roof to the trailer roof. The front corners are well rounded and have a channel to guide the flow around the corners. Though, it should be said that these devices are the only ones present on the tested vehicle. There are no side skirts, neither on the truck or the trailer, and the trailer has not a boat tail or some other kind of drag reducing device mounted.

In Figure 5 the corresponding surface model for the truck and the trailer is demonstrated. The external features of the model are well defined, in order to obtain realistic results from the simulations.

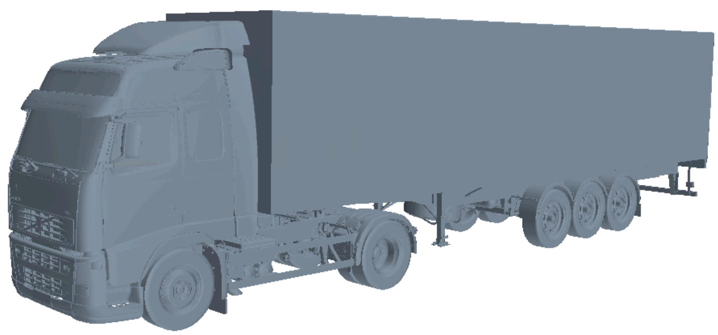

Figure 5: Surface model of the truck and trailer

In order to obtain results that are realistic and correspond to as real-life situations as possible, the model of the cooling system also has to be well defined. A high resolution of the cooling package is a necessity for simulations where the cooling system is such an important part. A schematic picture of the cooling system set-up with AC condenser, CAC and radiator can be seen in Figure 6. The part placed in the front is the AC condenser, the middle part is the CAC and the rear part is the radiator.

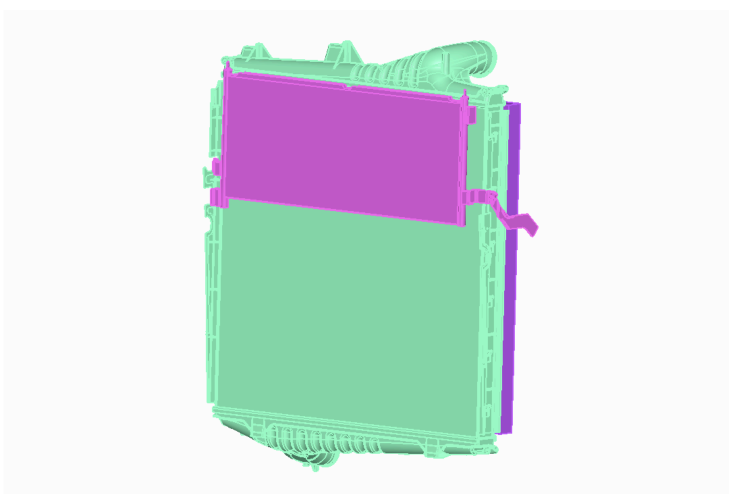

Figure 6: The cooling package seen from the front with a slight angle

In the following subsections the cases that will be evaluated are presented. It is important to have in mind that these air restriction designs will only be used when it is desired to limit the cooling airflow.

3.1 Opened splitline

In the main task, five different geometry set-ups of the truck and trailer are to be analyzed. The first case corresponds to the Volvo FH16, which is on the market today, with no coverage of grill or the cooling system. This case is also defined as the reference case in this research. The four remaining cases have either a covered grill or a covered cooling package that is either fully or intermediately covered. The aim for having the grill or cooling package fully covered is to obtain the minimum aerodynamic resistance for the vehicle. This is based on research carried out by Kuthada et al [6], who claims that the aerodynamic resistance will be increased when having airflow through the underhood area. Though, since it is often desired to have air condition active inside the cab compartment the cases with intermediate coverage up to the AC condenser of the grill or cooling system are also tested. By having these two different coverage methods the aim is to find a preferable way of limiting the airflow into the cooling system depending on which method that yields least drag.

The case with intermediately covered grill and the case with totally covered grill are intended to be included in the same technical solution. It will then be possible to have totally closed, intermediate closed or opened grill. Reversely, the technical solution for a covered cooling package is also intended to function both for full and intermediate coverage of the cooling package. This solution makes it possible to have different amounts of air into the cooling system depending on the driving conditions.

The case set-up with proper numbering and descriptions can be seen in Table 1.

Table 1: Case set-ups

Case #	Description
1	No coverage of grill or cooling system, reference case
2	Grill covered 100%
3	Grill covered up to AC condenser
4	Cooling system covered 100%
5	Cooling system covered up to AC condenser

To illustrate the five geometry set-ups that are analyzed, Figure 7 and Figure 8 can be studied. In Figure 7, the reference case is shown, where no adjustments of the cooling air intake area are made. In Figure 8, the different cases where the cooling air intake area is restricted are shown.

Figure 7: Case 1, opened splitline - reference case

(a) Case 2 - grill covered 100%

(b) Case 3 - grill covered up to AC condenser

(c) Case 4 - cooling package covered 100%

(d) Case 5 - cooling package covered up to AC condenser

Figure 8: Case 2-5, restricted cooling air intake area with an opened splitline

As can be seen in the figures above the splitline is opened, just as it is at the vehicles in production today. The splitline is the horizontal opening between the cab and the chassis, which is the gap seen in the figures. These configurations make the main task of the research. As also can be noted from Figure 7 and Figure 8, the external features of Case 1, Case 4 and Case 5 are exactly the same. This is due to the fact that Case 4 and Case 5 represent full and intermediate coverage of the cooling package, which can not be seen in these figures. Figure 9 can be used to clarify the design of the air restriction for Case 4 and Case 5. The red color illustrates that no air can flow through this wall. Figure 9a represents Case 4, the fully covered cooling package, while Figure 9b represents Case 5, with covered cooling package up to the AC condenser.

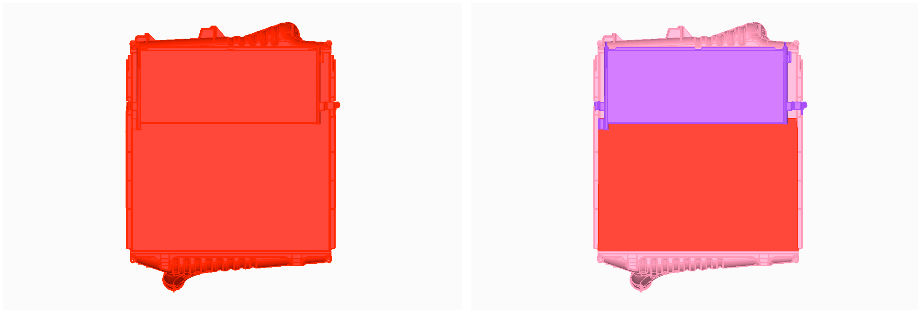

(a) Case 4, fully covered cooling package (b) Case 5, cooling package covered up to AC condenser

Figure 9: Cooling package configurations of Case 4 and Case 5

3.2 Closed splitline

The five different geometry set-ups which are described in Chapter 3.1 are also tested with a closed splitline. This is performed since it could be interesting to investigate the possibility of reducing drag by covering this gap. The space between the cab and the chassis is known to create a major vortex on each side of the cab. It would therefore be interesting to investigate if there are any differences in the flow field when covering the gap.

The modified geometry set-ups that are created to obtain the covered splitline can be seen in Figure 10. Note that the splitline is entirely covered in all five cases; compare with Figure 7 and Figure 8. Also note that design of the air restriction for Case 4 and Case 5 at the cooling package is the same as for the corresponding opened splitline cases.

(a) Case 1, closed splitline

(b) Case 2 - grill covered 100%

(c) Case 3 - grill covered up to AC condenser

(d) Case 4 - cooling package covered 100%

(e) Case 5 - cooling package covered up to AC condenser

Figure 10: Case 1-5, restricted cooling air intake area with a closed splitline

3.3 Yaw angle

Finally, all the above described case set-ups are to be tested with the wind flowing with first 0° yaw angle and then with a yaw angle of 5°. In Figure 11 the wind direction inside the wind tunnel with the truck and trailer model is demonstrated for 5° yaw angle. The reason why testing the vehicle with a 5° yaw angle is to ensure that the trends and magnitudes of the simulation results are realistic even with a yaw angle.

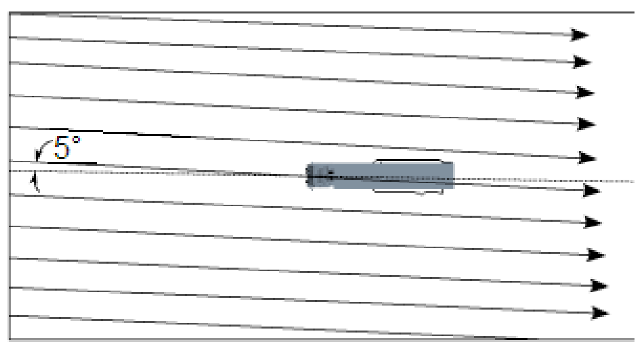

Figure 11: Wind tunnel with the air flowing with 5° yaw angle

Normally when testing the aerodynamics of heavy trucks with yaw angle, a sweep from -10° to +10° with a number of discrete steps in between is tested, and after the sweep a so called wind-averaged drag coefficient can be calculated. Due to the limited time, the number of simulations is narrowed down to only 5° yaw. This decision can be motivated by the fact that when a vehicle is driving on a road under normal conditions, it is known that the vehicle is subjected to an average wind with a yaw angle of approximately 5°. Therefore, it could be motivated to choose this angle for the simulations.

4 Case setup and procedure

In this chapter the procedure of this research is presented.

Initially, the design of the Volvo FH16 and the cooling package is studied, both by examining CAD models and drawings and by studying the physical truck in the workshop.

Two $3D$ models are given, one of the truck and one of the trailer, which are used to create the reference model. These two models are used since they both have detailed external and internal features. This is a necessity, since the calculations are intended to cover both total drag values and the airflow through the cooling system. A too rough model of the truck or the cooling system would result in a less accurate and reasonable solution compared to a real truck.

The process of generating the different case setups for the simulations is similar. The only thing which differs between the cases is a few settings in the softwares. Therefore, only the overall procedure of the research is described.

4.1 ANSA

The first step in the process of generating a complete truck and trailer model is to use existing CAD and FE models in the software ANSA. The truck and trailer are initially two separate models, which have to be merged into a single model. This is done by defining at which coordinates the two models should be joined.

To be able to simulate the airflow around the model a wind tunnel has to be created in ANSA. The simulated wind tunnel is representing the calculation domain, where a volume mesh will be created later on. The choice of size of the tunnel is made in correlation with CFD specialists within the field of external aerodynamics at Volvo 3P. The dimensions of the wind tunnel can be seen in Table 2.

Table 2: Wind tunnel dimensions

Wind tunnel	Dimension $[m]$
Length (x)	135
Width (y)	33
Height (z)	20

In Figure 12 the outline of the truck and trailer in the wind tunnel is displayed.

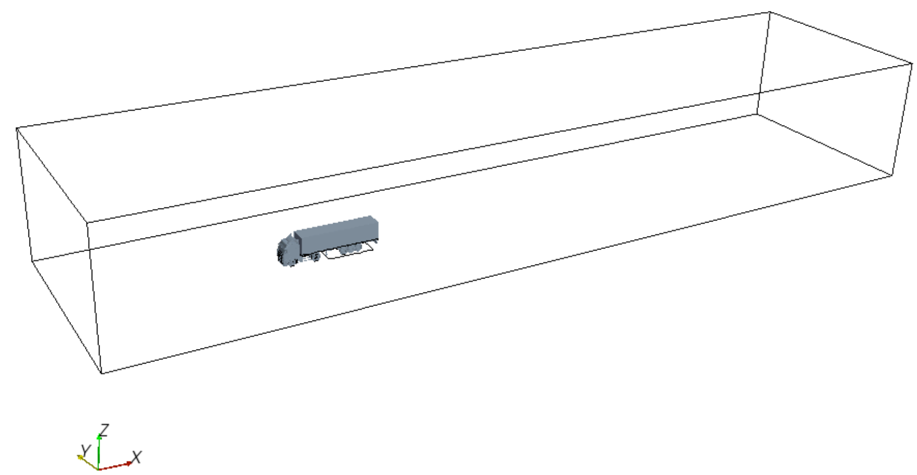

Figure 12: Truck and trailer model in the wind tunnel

The simulated wind tunnel used in this project is rather large, in order to capture all the flow effects around the vehicle. An important factor to avoid is the blockage effect, which is significant if the width and height of the wind tunnel are small in relation to the model. The walls of the tunnel will then affect the flow around the vehicle and thereby affect the numerical results from the simulations. Since the tunnel is somewhat over dimensioned in this case the blockage effect will be small. The distance from the rear end of the trailer to the wind tunnel outlet is fairly long, in order to capture the entire wake structure behind the vehicle. A wake is produced when the adverse pressure gradient of the flow becomes too large so that the airflow no longer stays attached to the surface. These wake areas are recognized by low pressure and turbulence [3].

In the pre-processing software smaller geometrical changes are made to the models. For all cases the deflector angle is changed to better fit the height of the trailer. When it comes to changing the geometry of the grill or cooling system for each case, it is also performed in ANSA. The geometrical changes that are made for each case are presented in Chapter 3.

Before exporting the file to StarCCM+, a surface mesh is applied to the model. In ANSA, it is possible to receive a surface mesh either by surface meshing or wrapping. Both methods results in a mesh, but in different ways. In this case, the two models of the truck and the trailer origins from different sources and are both a mix of CAD data and FE data. This results in a merged model with both meshed and wrapped surfaces. As long as there is some kind of surface mesh on the model, it does not matter if the model is wrapped or meshed, StarCCM+ can still generate a proper surface remesh later on.

ANSA is furthermore used to set different Property Identifications (PID's) to different parts of the model. By dividing the model into several PID's the further work is simplified substantially. The largest advantage with having several PID's is that the model turns out to be well structured. Another advantage is that it is possible to set different cell sizes on separate PID's when further working in StarCCM+. Also, if the wheels of the model should be rotating, it is a necessity to set these parts as separate PID's. This ANSA model is divided into approximately 50 PID's.

When the geometrical changes are made and a surface mesh is generated, the last step in ANSA is to export the file to a format suitable for StarCCM+. In this case the files in ANSA are exported as Star CD files.

4.2 StarCCM+

The work in StarCCM+ starts with importing the output file from ANSA. In StarCCM+, the model can be divided into several regions if different set-ups are required for different parts of the model. The model exported from ANSA is divided into four regions; the first containing the vehicle model and the wind tunnel excluding the cooling package, the second including the CAC, the third the AC condenser and the fourth including the radiator. The reason why dividing the cooling package into three parts is that it consists of porous media where the values of the inertial and viscous resistance differs between the cooling system components. It is of great importance that these values are set correctly, in order to obtain a cooling system that is as similar the real one as possible.

Another reason why separating the region for the truck and trailer from the cooling package is that the coordinate systems for these two regions does not coincide. The cooling system is slightly tilted backwards, with an angle of approximately 4°. Therefore, a new coordinate system is created in StarCCM+ which suits the cooling system. It is then applied to the regions for the CAC, the AC condenser and the radiator.

In order to connect the three cooling system regions to the region where the rest of the truck and trailer is situated, a few interfaces are created. One interface is created between the inlet of the AC condenser and the core of the AC condenser and a similar one is created between the outlet of the AC condenser and the core of the AC condenser. The inlet of the AC condenser is placed in the region for the truck and trailer while the core of the AC condenser is placed in the region for the AC. Similar interfaces are created in the remaining regions for the CAC and radiator.

What also have to be determined are which solver settings that should be used. First, the type of fluid that is flowing in the domain and its properties should be set. Also, the flow characteristics has to be defined; for example if the flow is stationary or non-stationary, two-dimensional or three-dimensional etc. The choices of solver settings are made in correlation with CFD experts at Volvo 3P and are considered suitable for the type of simulations that are treated in this research. The complete list of solver settings is shown below.

- Three-dimensional turbulent flow
  - the flow field has velocity components in the x-, y- and z-direction
- Stationary flow
  - the flow is considered as non-transient; the flow is not varying over time
- Gas: air
  - density: $1.18415\, kg/m^3$
  - dynamic viscosity: $1.85508\, Pa/s$
- Segregated flow
  - the connection between the pressure and velocity is weak. The equations for these parameters can be solved separately.
- Incompressible flow
  - the density of the air is constant
- Reynolds-Averaged Navier-Stokes (RANS)
  - to obtain the RANS equations, the Navier-Stokes equations for the instantaneous pressure and velocity fields are separated into a mean value and a fluctuating component. For steady-state situations, the process may be considered as time-averaging. The resulting equations for the mean quantities are basically identical to the original ones, except for an additional term that occurs in the momentum transport equation. The additional term is known as the *Reynolds stress tensor*, which is modeled with the $K\epsilon$ turbulence model.
- Realizable $K\epsilon$-turbulence model
  - the $K\epsilon$ model is a two-equation turbulence model, which means that two extra transport equations are added to characterize the turbulent properties of the flow. K represents the turbulent kinetic energy, whereas ϵ represents the turbulent dissipation. The realizable $K\epsilon$ model contains a new transport equation for the turbulent dissipation rate ϵ, which is not included in the standard $K\epsilon$ model [2].

- Two-layer All y^+ Wall treatment
  - the two-layer approach allows the $K\epsilon$ model to be applied in the viscous sublayer. The viscous sublayer is divided into two layers where the computations are performed. In the layer closest to the surface, the turbulent dissipation rate and the turbulent viscosity are specified as functions of wall distance. The values of these properties are blended smoothly with the values computed from solving the transport equation far away from the wall.
- Cell quality remediation
  - this model can be applied in order to obtain solutions on meshes with poor quality. The model identifies poor-quality cells based on certain pre-defined criteria, for example skewness angle that exceeds a threshold value. When the cells with poor quality and their neighbour cells have been identified, the computed gradients in these cells are modified in order to improve the robustness of the solution.

To obtain the desired resolution of the model, each pre-defined PID from ANSA is set to a specific value of the surface cell size. A high resolution of the surface model will result in a more accurate solution, though this will result in a larger volume mesh which in turn yields a heavier calculation. The choice of cell size is a trade-off between computer power and simulation accuracy. The choices of surface cell sizes are carried out with supervision from CFD experts at Volvo 3P.

A few settings for the volume mesh are defined at this stage, since these settings also affect the build-up of the surface mesh. These settings are the *volume sources* and the *prism layers*.

In certain flow field areas where a higher resolution is desirable, so-called *volume sources* can be placed in which a fixed cell size can be set. In this truck and trailer model, these volume sources are located around the air deflector, at the gap between truck and trailer, at the grill surface, at the wheels near the ground and at the wake behind the trailer. The last mentioned volume source is divided into three boxes with different cell sizes; the cells will grow gradually as moving from the object towards the wind tunnel walls. The truck and trailer model including the volume sources is presented in Figure 13.

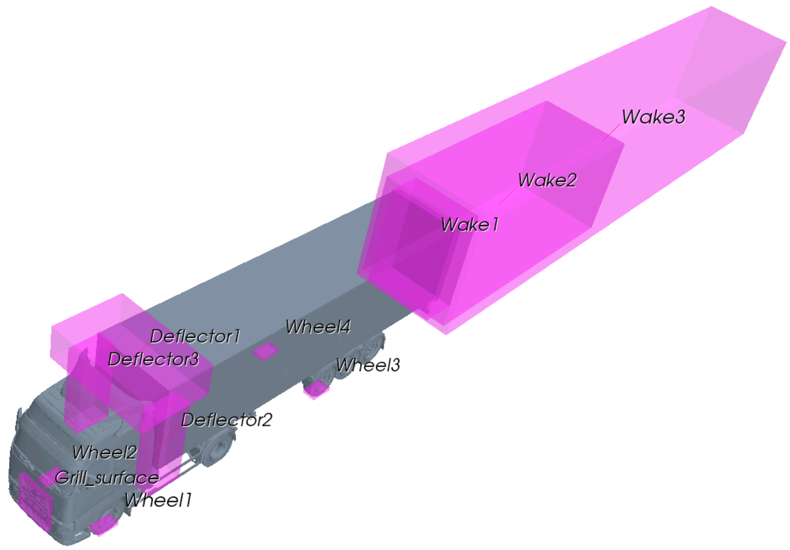

Figure 13: Truck and trailer with defined volume sources areas

Closest to the vehicle surface a *prism layer* is added which means that thinner volume cells are used. It is recommended to use prism layers around the vehicle in order to resolve the boundary layer properly. An ordinary volume cell, which has the same length of each side, is not proper to use at the surface since the resolution of the flow will be too low and the simulation will be inaccurate. To generate a realistic solution of the flow closest to the surface it is recommended that the $y+$ value should be between $30 - 100$. $y+$ is a dimensionless wall distance parameter which in CFD can be used to predict the accuracy of the solution. If the $y+$ value is outside the interval mentioned above the pre-defined equations will not be adequate to simulate real conditions. However, since the *All* $y+$ *wall treatment* method is used, the model will still be acceptable from an accuracy point of view for $y+$ values below 30.

Figure 14 shows the surface of the vehicle in a side view with two prism layers closest to the surface, which is transformed to ordinary volume cells as moving towards the wind tunnel walls. The thickness of the two layers is $4\,mm$ in total and is constant over the entire vehicle surface. The inner prism layer is thinner than the outer one.

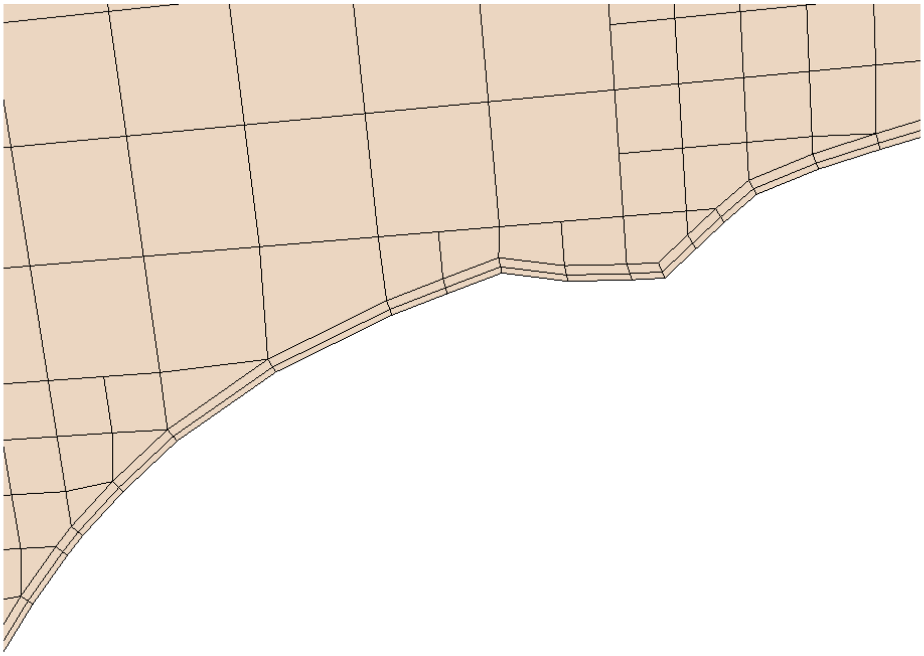

Figure 14: Prism layers in the volume mesh near the vehicle surface

It is of great importance for the solution of the simulation that the boundary conditions for the entire model are reasonable. In this research, the truck and trailer is simulated with a moving ground and rotating wheels in order to achieve driving conditions that are similar to the real driving case. A complete list of the boundary conditions for the entire model with 0° yaw is shown in Table 3. The truck and trailer is in this table merged into one part, except for the wheels and the cooling package where different boundary conditions should be applied. The vehicle is driving straight forward with a velocity of 90 km/h with the wind flowing with 0° yaw and thereafter 5° yaw for the different cases. It should be clarified that the two rearmost wheel couples for the trailer are not rotating since these wheels are not in contact with the ground.

Table 3: Boundary conditions for the model

Part	Type of boundary condition
Truck & trailer	Stationary wall
Front wheels - truck	Moving wall - local rotation rate
Rear wheels - truck	Moving wall - local rotation rate
Front wheels - trailer	Moving wall - local rotation rate
Middle wheels - trailer	Stationary wall
Rear wheels - trailer	Stationary wall
CAC inlet main	Internal interface boundary
CAC outlet main	Internal interface boundary
Condensor inlet main	Internal interface boundary
Condensor outlet main	Internal interface boundary
Radiator inlet main	Internal interface boundary
Radiator outlet main	Internal interface boundary
Ground	Moving wall - wall vector
Inlet	Velocity inlet
Outlet	Pressure outlet
Top	Symmetry plane
Left wall	Symmetry plane
Right wall	Symmetry plane

For the simulations run with 5° yaw the boundary conditions for the right and left wall of the wind tunnel are set to *velocity inlet* instead of *symmetry plane*. This setting is applied since the air is entering the wind tunnel with a slight angle.

Before the surface mesh generation can be performed the four regions defined in the beginning of this subsection have to be separated into four different mesh domains. This has to be done since the regions uses different coordinate systems; the solution will be more accurate and the mesh will be of higher quality if the meshes inside the cooling package regions are tilted. When the regions are divided into four mesh domains, the surface mesh generation can start.

The surface mesh generation process in this case consists of both surface wrapping and surface remeshing. The wrapping process is carried out to cover all potential small holes in the CAD and FE model in order to receive a solid surface of the entire model. If the small holes in the geometry are not covered StarCCM+ will generate a surface mesh on the inside of the hole as well, which will result in a large increase of the amount of surface cells. The wrapping process is directly followed by the surface remeshing, where a mesh is applied to the model surface. The software creates a mesh that fulfils the requirements regarding cell sizes on different parts, both for the truck and trailer model but also for the volume sources that cuts the model surface. The amount of surface cells will depend on the settings of the surface size that were done earlier in the process. The surface remeshing is an iterative process; in this research the surface meshing is repeated several times in order to obtain a reasonable amount of surface cells, and also to achieve an acceptable resolution of the model. The final amount of surface cells is in the order of 3.9 million cells for all cases.

The surface meshing process is followed by the volume meshing. The software generates a volume mesh based on the surface mesh, the defined volume sources and the added prism layers. Also, the volume cells are set to be increasing in size as moving towards the wind tunnel walls. This can be considered to be a proper method since the flow at the tunnel walls is almost not affected by the vehicle model, and it is therefore not necessary to solve the flow more exact at this location. A *trimmer mesh* is applied to the model, which means that a quadrangular volume mesh is aimed for. Most of the cells are quadrangular, but as the cells cut the vehicle model surface they are transformed to different shapes. This means that the mesh will consist of different shapes of the volume cells, but the majority of the cells will be quadrangular while just a few will have different shapes. The total number of volume cells is approximately 21.3 millions for each case. When the volume mesh is created it can be checked against quality criteria to make sure that most of the cells are accurate enough to be able to run a simulation. The cells that are unacceptable can be deleted; in these cells there will not be any results from the simulation. As long as the number of invalid cells does not exceed several hundreds or the location of these cells is not at places where a high resolution is desired, it is acceptable to delete these cells.

When the volume mesh is generated and all invalid cells are deleted the simulation can be started. The simulations are run for approximately 3000 iterations before the solutions are considered as converged. Some cases demanded more iterations to converge, but 3000 iterations can be considered as some kind of guideline. The convergence is checked by controlling the plots for the residuals and the C_d value. When the values of the drag coefficient and the residuals are approximately constant from iteration to iteration, the solution is said to have reached convergence. The time for performing a simulation is depending on the number of cells for the model and how fast the solution converges. A higher amount of volume cells will naturally prolong the simulation time. The simulations in this research are running for approximately 10-14 hours on 28 or 32 cores before the solution is converged.

The post-processing part of the work is also carried out in StarCCM+. In this research, values of the drag coefficient and the mass flow of air through the different parts of the cooling system are considered as important properties. Pictures of the pressure field and the velocity field around the truck and trailer are extracted and used for the analysis part of the work.

The process of generating a complete model as is described in this section is done once for the reference model. For the remaining cases, the same settings in StarCCM+ are used, the only difference is that the design of the grill or the cooling package is exchanged from case to case. The simulation process can be automated, by running scripts that reads output files from ANSA and applies the same settings as a pre-defined reference simulation file and runs the simulation. By using this method a lot of time is saved, and the risk of applying wrong or different settings to the different cases is eliminated.

5 Results

In this chapter, the results from the CFD simulations are presented. The parameters that are extracted from the simulations are the averaged C_d values and the values of the mass flow of air through the different parts of the cooling system. The average C_d value is calculated by using the C_d graph generated from the simulation, when the solution is said to be converged. By adding the maximum and minimum C_d value from the graph for each case and dividing this value with two, the average C_d value is obtained. The variation of the C_d value when the solution is said to be converged is also presented. The extra power required to overcome the aerodynamic resistance for the truck and trailer is presented in the results for each geometry set-up. The percentage change of C_d in relation to the reference case and the drag counts versus the reference case are also presented in this chapter. The mass flow of air through the AC condenser, the CAC and the radiator are presented in order to detect differences or similarities for the cases when covering either the grill or the cooling package of the vehicle. Figures showing the pressure and velocity distribution at the vehicle surface and around the vehicle are also presented, together with figures of isosurfaces.

As mentioned in Chapter 4 the $y+$ value is recommended to be in the range between 0 and 100 in order to receive accurate results. The $y+$ value for the reference case is presented in Figure 15. As can be seen in the figure the $y+$ value is between the recommended limits for almost the entire model. There are only a few areas in the flow field where the $y+$ value is above the recommended upper limit, and for this research the results will still be seen as accurate.

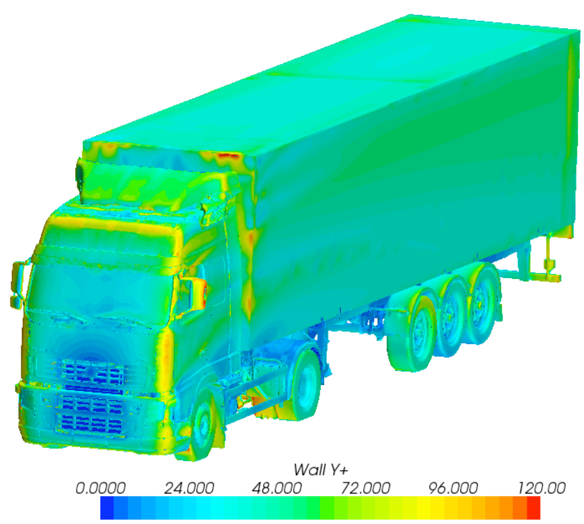

Figure 15: $y+$ value over the entire vehicle surface for the reference case

In the following subsections, the results from the simulations for Case 1 to Case 5 are presented, both for the cases with opened and closed splitline. The results presented until Chapter 5.5 are valid for the simulations run with 0° yaw.

5.1 Aerodynamic resistance and mass flow

In Table 4 the results from the simulations with opened splitline are displayed. The parameters shown are those that are described above, and in the rightmost column the reduction in drag counts compared to the reference case is presented. Case 1 with opened splitline is synonymous with the reference case, since this design corresponds to the vehicle in production today. The configuration of each case number is presented in Chapter 3. The range within which the C_d value varies, shown in the third column in the table, are low for all cases which indicates that the solutions have converged well. This trend is also seen for the remaining simulation results.

Table 4: Aerodynamic drag and required power for the opened splitline cases

Case #	C_d	C_d +/-	Power [kW]	% change of C_d vs ref. case	Drag counts vs ref. case
1	0.467	0.00175	45.93	0.0	0
2	0.450	0.00130	44.24	-3.7	-17
3	0.463	0.00175	45.56	-0.8	-4
4	0.454	0.00125	44.67	-2.7	-13
5	0.458	0.00150	45.10	-1.8	-8

By analyzing the parameters in the table above it can be stated that all four modifications of the original truck geometry results in a reduction in drag. It can be seen that the highest aerodynamic drag is achieved for the reference case which has a drag coefficient of 0.467, whereas the largest reduction in drag is seen for Case 2, the case with 100% covered grill area. Case 2 has a C_d value that is lowered with 17 drag counts compared to the reference case. In other words, the drag coefficient is lowered by 3.7% when having a fully closed grill area with an opened splitline. Translating this drag reduction into reduction in fuel consumption, results in a decrease of almost 1.3%. The same magnitude of the drag reduction can not be seen when covering the cooling package 100%; this configuration only results in a decrease with 13 drag counts and with a decrease of 0.9% in fuel consumption. Case 3 and Case 5, which have an intermediate covered grill and cooling package, only show a decrease of 4 and 8 drag counts respectively. Case 3 results in a reduction in fuel consumption with almost 0.3% and the corresponding value for Case 5 is 0.6%. Though, the two cases with 100% covered grill or cooling package are more favourable from a drag coefficient point of view, compared to intermediate coverage of the grill or cooling system.

The values of the mass flow of air through each part of the cooling system for the cases with opened splitline are presented in Table 5.

Table 5: Mass flow of air through each part of the cooling system for the opened splitline cases

Case #	$\dot{m}_{AC}$ $\left[\frac{kg}{sec}\right]$	$\dot{m}_{CAC}$ $\left[\frac{kg}{sec}\right]$	$\dot{m}_{radiator}$ $\left[\frac{kg}{sec}\right]$
1	0.893	3.273	2.950
2	0.465	0.907	0.751
3	1.204	1.646	1.451
4	0.000	0.000	0.000
5	1.142	1.560	1.459

Analyzing the table above, it is clear that Case 1 has the highest amount of air that passes trough the CAC and the radiator. Though, the amount of air flowing through the AC condenser is larger for Case 3 and Case 5, compared to the reference case.

Naturally, Case 2 and Case 4 have the lowest airflow through the cooling package, since these cases have a fully closed grill or fully closed cooling package. However, the mass flow of air through the cooling system for Case 2 is still quite substantial. It should be noticed that the splitline is opened in this case and air can enter the cooling system from here.

When comparing the C_d values in Table 4 and the mass flow of air in Table 5 it is seen that there is a relationship between the different parameters. A low mass flow of air through the cooling system contributes to a low C_d value for these cases.

The results from the simulations for Case 1-5 with a closed splitline are presented in Table 6.

Table 6: Aerodynamic drag and required power for the closed splitline cases

Case #	C_d	C_d +/-	Power $[kW]$	% change of C_d vs ref. case	Drag counts vs ref. case
1	0.461	0.00150	45.37	-1.2	-6
2	0.434	0.00180	42.70	-7.0	-33
3	0.448	0.00140	44.09	-4.0	-19
4	0.450	0.00160	44.32	-3.5	-16
5	0.451	0.00100	44.40	-3.3	-16

The C_d values for the cases with closed splitline are all lowered compared to the C_d values for the corresponding case with opened splitline. It can also be said that all five cases simulated with a closed splitline results in a lower C_d value than for the reference case. Case 2 has the lowest C_d value compared to the remaining cases for both opened and closed splitline. Compared to the reference case the C_d value for Case 2 with closed splitline is lowered with almost 33 drag counts, which corresponds to a fuel consumption reduction of 2.3%. Both whole and intermediate coverage of the grill generate a lower C_d value than covering at the cooling package. It is seen from the table above that an intermediate covered grill generates a drag reduction of 19 drag counts, while an intermediate covered cooling package only is reduced with 16 drag counts compared to the reference case. Case 3 with closed splitline has a fuel consumption reduction of 1.3%.

It is worth noticing that Case 4 and Case 5 have the same reduction in drag counts, even though they have different coverage degrees of the cooling system. The fuel consumption reduction for these two cases is almost 1.2%.

The mass flow of air through the parts of the cooling package is presented in Table 7.

Table 7: Mass flow of air through each part of the cooling system for the closed splitline cases

Case #	$\dot{m}_{AC}\left[\frac{kg}{sec}\right]$	$\dot{m}_{CAC}\left[\frac{kg}{sec}\right]$	$\dot{m}_{radiator}\left[\frac{kg}{sec}\right]$
1	0.671	3.050	2.731
2	0.005	-0.001	-0.035
3	0.990	1.101	0.949
4	0.000	0.000	0.000
5	0.909	1.390	1.350

The amount of air that passes through each part of the cooling package for these cases is slightly lower than for the cases with opened splitline. Case 2, which has the lowest C_d value, has no air that flows through the cooling system since the splitline is closed, there is just some air recirculation. As a conclusion; both the aerodynamic drag and the airflow through the cooling system are reduced for all cases with closed splitline compared to the same case with opened splitline.

To be able to draw any conclusions about the influence of a closed splitline, each opened splitline case has to be compared with its corresponding closed splitline case. In Table 8 the drag counts change for the corresponding opened and closed splitline cases are shown. A negative value of DC_{change} indicates that a closed splitline tends to lower the C_d value.

Table 8: Drag counts change between each case with opened and closed splitline

Case #	DC_{change}
1 closed - 1 opened	-6
2 closed - 2 opened	-16
3 closed - 3 opened	-15
4 closed - 4 opened	-4
5 closed - 5 opened	-7

From the table above it is seen that Case 2 and Case 3 are the cases that are most influenced by the closed splitline.

5.2 Pressure distribution

Figure 16 displays the static pressure on the vehicle surface seen in a front view for the reference case. The scale of the pressure reaches from $-800\,Pa$ to $430\,Pa$, where $0\,Pa$ represents the reference pressure which equals the atmospheric pressure, $101325\,Pa$, for these cases. This scale is used for the different pressure visualizations further on in the report.

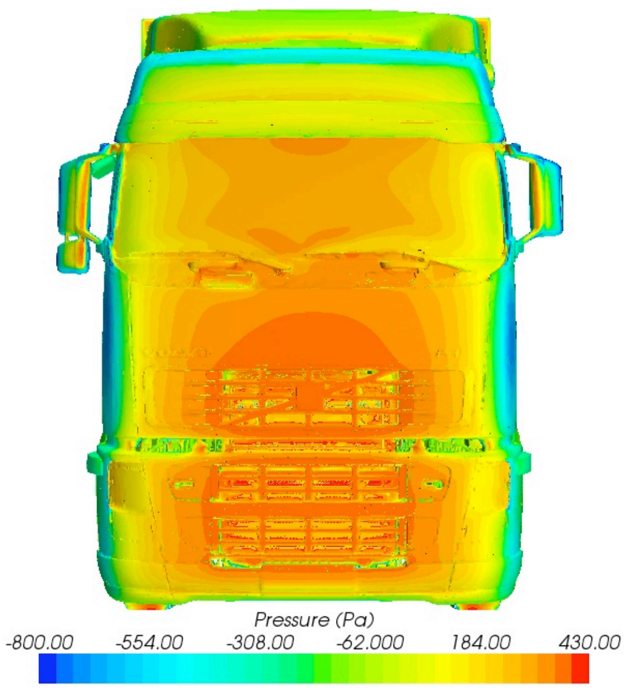

Figure 16: Surface pressure for the reference case, Case 1 with opened splitline

In the figure above, it is quite straightforward to detect the stagnation pressure area. The stagnation pressure area is defined as the area where the highest pressure occurs, according to Barnard [3]. In Figure 16, the area with the darkest orange colour represents the stagnation pressure area. Barnard [3] further states that the bigger pressure difference between the front and rear of the vehicle, the higher the aerodynamic resistance in terms of pressure drag will be produced. In Chapter 2 it is stated that high pressure regions have low velocities, due to the Bernoulli equation. Hence the lowest velocity, which is equal to $0\,m/s$, occurs at the stagnation area. From Figure 16 it can then be stated that the highest velocities occurs at the front edges of the truck and at the deflector.

The pressure distribution structure in front of the vehicle is of great importance for the aerodynamic resistance. The centerline pressure in front of the vehicle and the pressure distribution seen from above, at a height of 1.5 meter above the ground, for the reference case are presented in Figure 17.

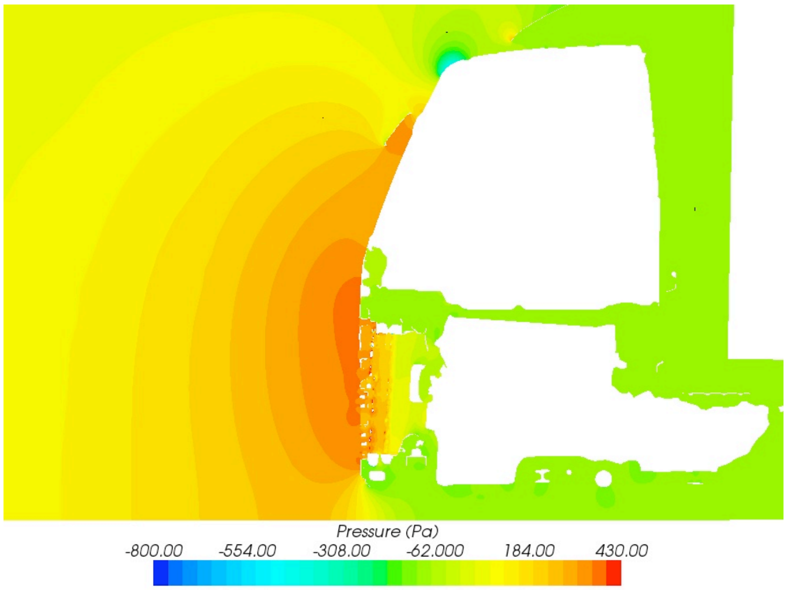

(a) Centerline pressure distribution

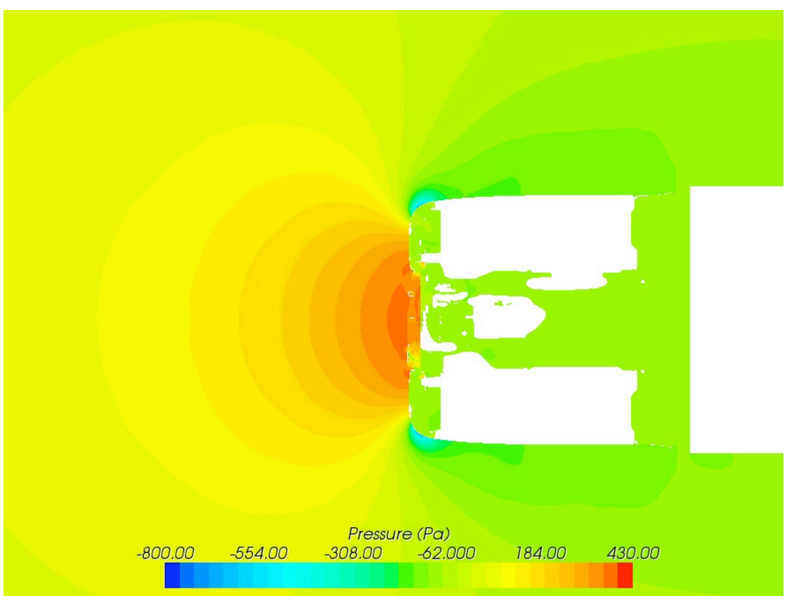

(b) Top view of the pressure distribution at the height z=1.5 m

Figure 17: Pressure distributions in front and above the vehicle for the reference case, Case 1 with opened splitline

Due to the high-pressure region the air in front and at the sides of the truck is affected. This is seen on the pressure rings in front of the vehicle in Figure 17a and in Figure 17b. By studying the centerline pressure distribution figures it is seen where the incoming air is flowing. In Figure 17a the air enters over the whole grill area and thereafter flows through the AC condenser, the CAC, the radiator and then towards the engine.

In Figure 18 the pressure distribution for Case 2 and Case 4 is shown in a front view. It is seen that the pressure fields for Case 4 are fairly equal to the reference case. Though, when comparing the pressure figure for Case 2 with the corresponding figure for the reference case, it can be seen that the stagnation pressure area is slightly reduced for Case 2.

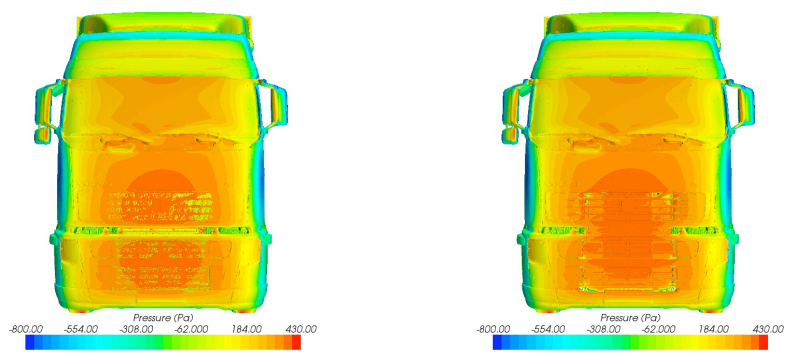

(a) Case 2, opened splitline (b) Case 4, opened splitline

Figure 18: Pressure distribution seen in a front view for Case 2 and Case 4 with opened splitline

The pressure distribution figures for the cases with closed splitline are approximately the same as the cases with opened splitline. The pressure distributions for each case in a front and side view are seen in Appendix A and in Appendix B.

5.3 Velocity distribution

Visualizing the flow field with figures of the velocity distribution gives an impression of how the air flows through the underhood area but also around the vehicle.

The velocity distribution for the vehicle in a centerline view is shown in Figure 19 for the reference case.

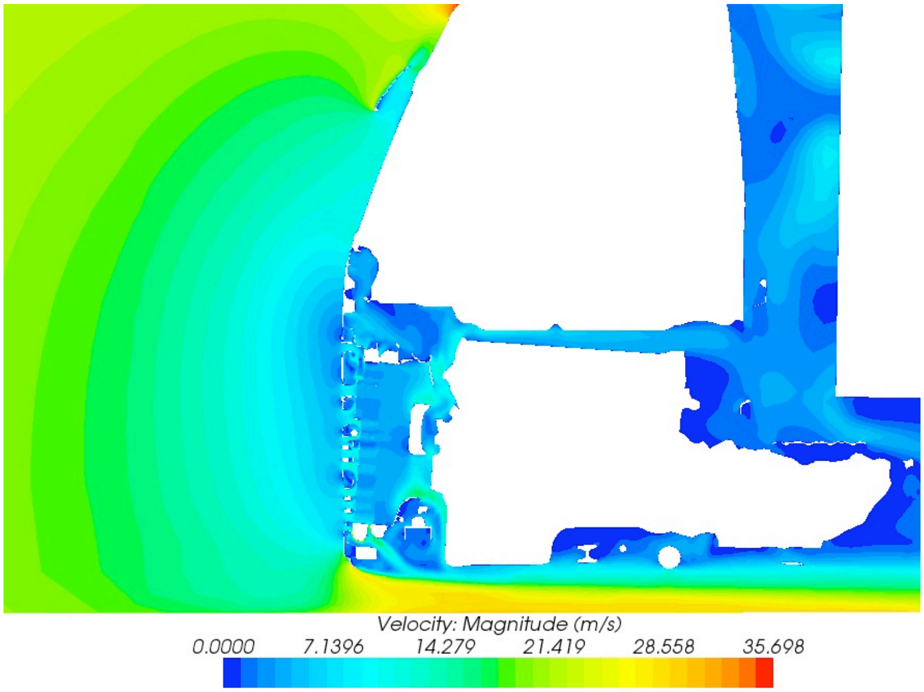

Figure 19: Velocity distribution shown from the centerline for the reference case, Case 1 opened splitline

It can be seen in the figure above that the airflow in the underhood compartment is significant. It can also be stated when viewing the figure that there is leakage of air between the CAC and radiator. This can also be confirmed by using the numerical results from Table 5 and Table 7; for all cases where there is air entering the cooling system, the amount of air going through the radiator is less than the air entering the CAC. This means that there is some kind of leakage at the upper and lower edge between the radiator and the CAC. In this figure it is not possible to decide if there is any leakage at the sides. By comparing the velocities in Figure 19 with the pressure filed in Figure 17a it is seen that where the stagnation pressure is situated the velocity is almost equal to $0\,m/s$, which the Bernoulli equation states. As can be seen in the figure above, at the back side of the grill there are some areas where the air recirculates.

In Figure 20, the velocity distribution seen from the centerline for Case 2 with both opened and closed splitline is seen.

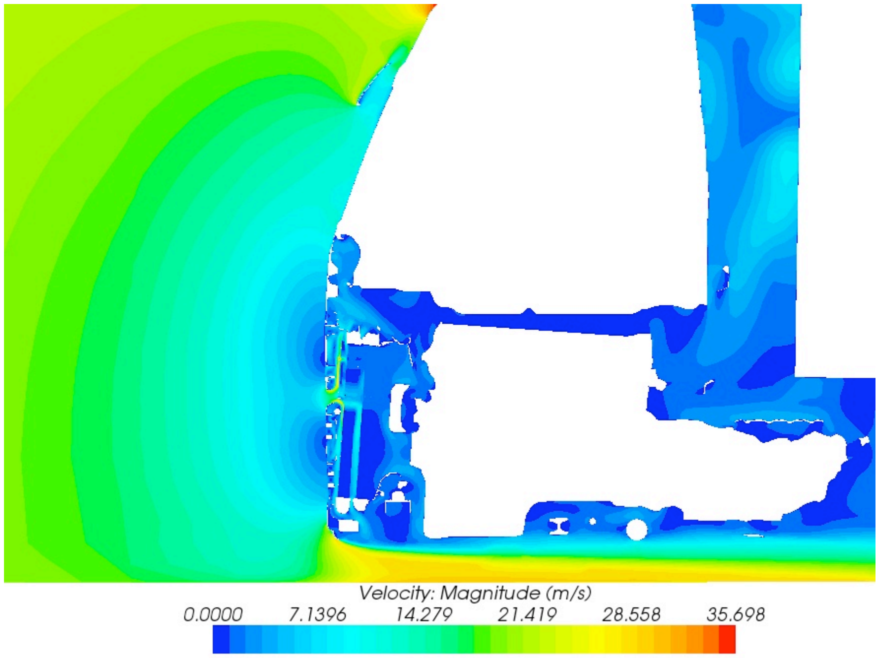

(a) Case 2, opened splitline

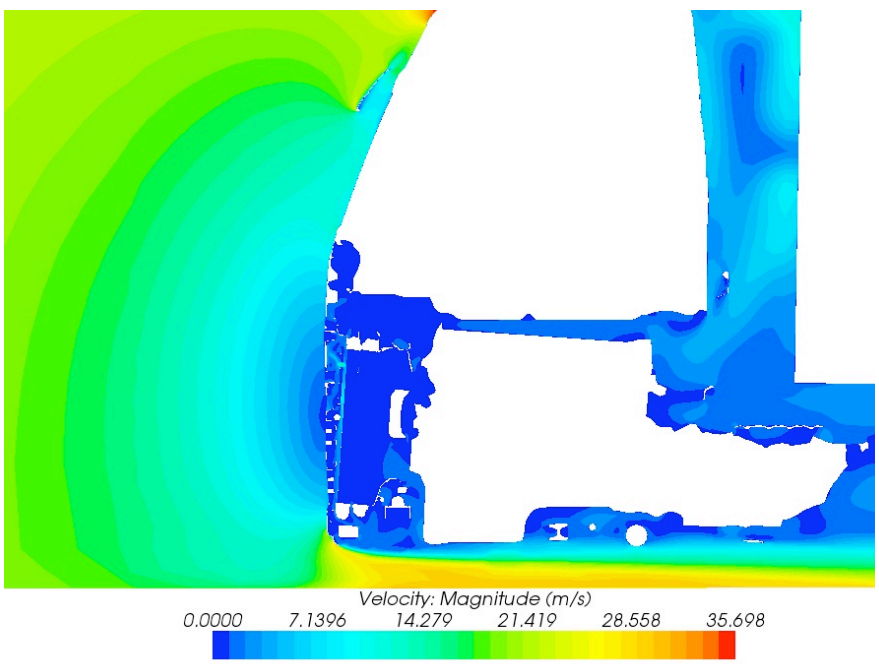

(b) Case 2, closed splitline

Figure 20: Velocity distribution shown from the centerline for Case 2 with opened and closed splitline

Analyzing Figure 20a it is evident that when having an opened splitline and a 100% covered grill the flow in the underhood compartment is extensive, even though the only opening into the cooling system consists of the splitline area. As also can be seen from Table 4, there is a significant amount of air flowing through the cooling system for Case 2 with opened splitline, and this is what can be observed in Figure 20a. When analyzing Figure 20b it is seen that the case with 100% covered grill and covered splitline has almost no airflow trough the cooling system. This can also be seen in Table 7.

In Figure 21, the velocity figures for Case 3 and Case 5 with opened splitline are shown. It can be stated when analyzing the velocity fields in the two pictures that there is air leakage for both cases. For Case 3 the air flows over the splitline opening and continues downwards and into the cooling package. For Case 5 the air flows through the grill and accelerates around the lower edge of the CAC and the radiator.

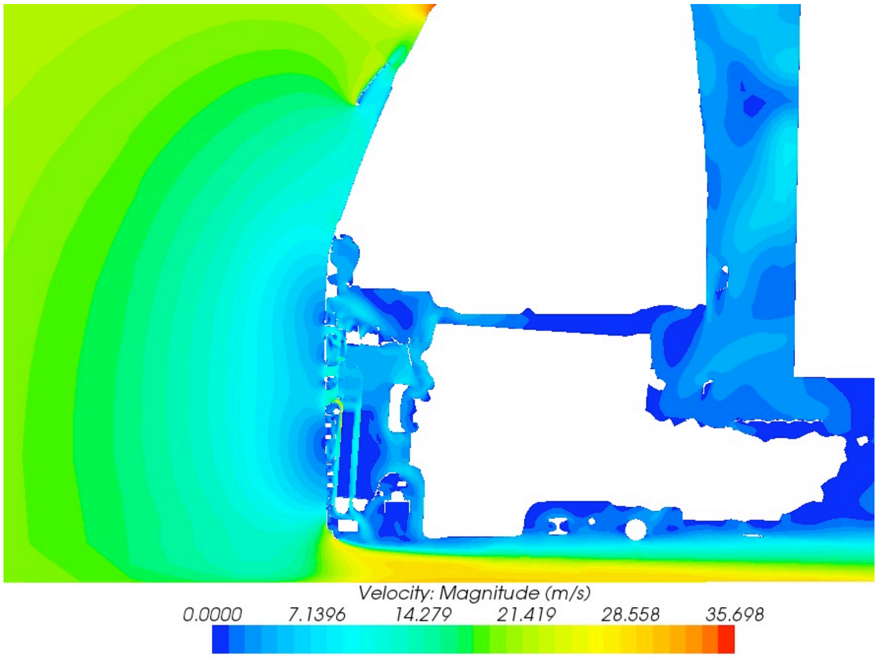

(a) Case 3, opened splitline

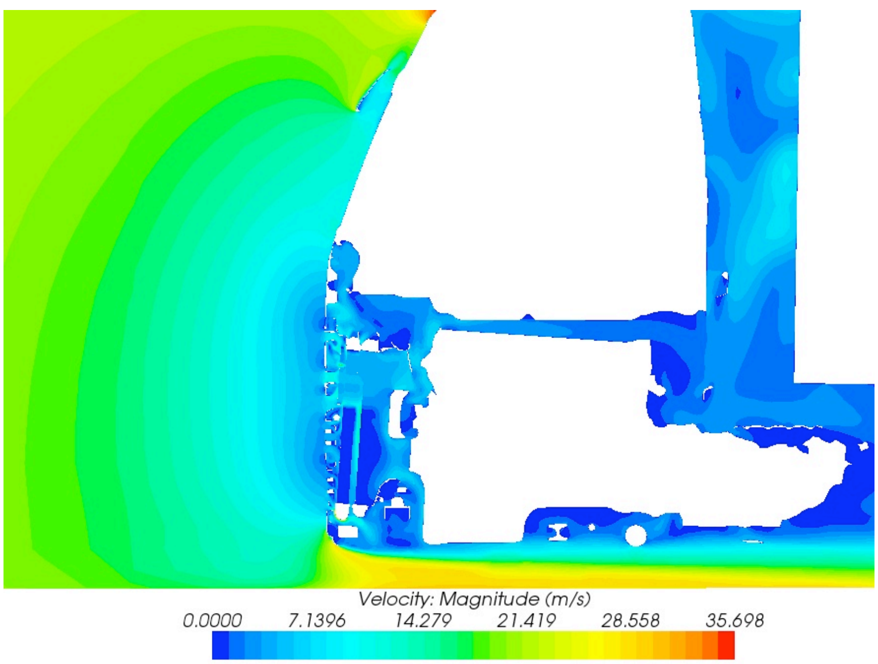

(b) Case 5, opened splitline

Figure 21: Velocity distribution shown from the centerline for Case 3 and Case 5 with opened splitline

The figures of the velocity distribution for the cases with 0° yaw angle not shown in this chapter are shown in Appendix E.

5.4 Isosurface figures

In Figure 22 a visualization of an isosurface where the total pressure equals zero is shown for the reference case. Figure 22a visualize the front view isosurface for the reference case while Figure 22b shows the side view of the model. The isosurface indicates regions where energy losses arise; mainly due to separation regions and turbulence. By changing the design of the vehicle the structure and size of these areas will be affected.

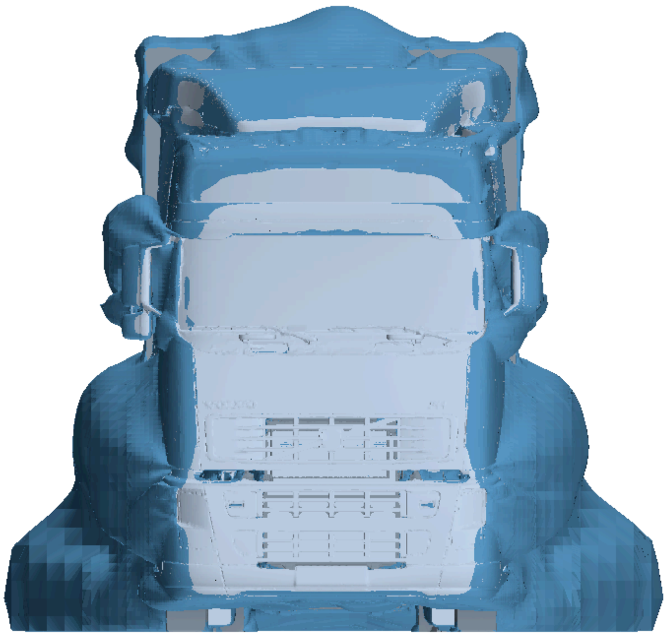

(a) Front view

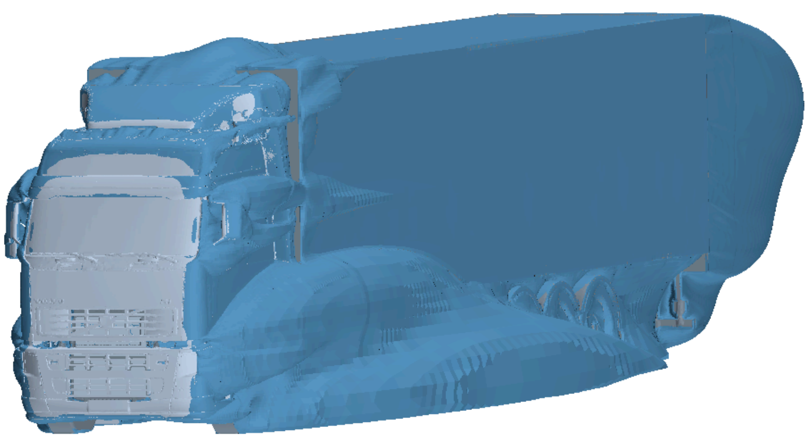

(b) Side view

Figure 22: Isosurface for the reference case, Case 1 with opened splitline

When analyzing Figure 22b it is clear that energy losses occur in the wake behind the trailer, but also at the wheels and at the rear view mirrors. There is also a large separated region which originates from the splitline and spreads along the sides of the truck. Smaller separation areas can be seen at the air deflector and in the splitline.

Figure 23 shows the isosurfaces for Case 1 with closed splitline.

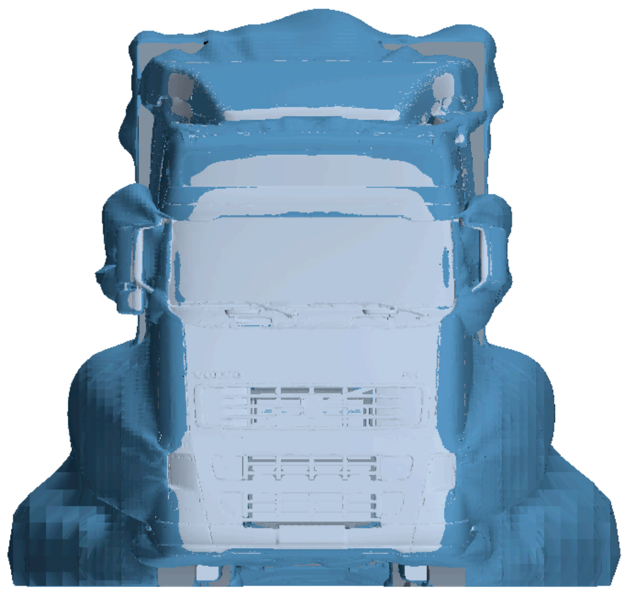

Figure 23: Isosurface front view for Case 1 with closed splitline

The difference between this case and the reference case is that the isosurface at the splitline is eliminated. The isosurface at the sides which originates from the splitline is also decreased.

5.5 5° yaw angle

Each above mentioned case has also been simulated with the wind coming 5° from the centerline of the vehicle. The parameters that have been presented in Chapter 5.1 for 0° yaw are also presented with 5° yaw in Table 9 and Table 10.

Table 9: Opened splitline

Case #	C_d	C_d +/-	Power $[kW]$	% change of C_d vs ref. case	Drag counts vs ref. case
1	0.613	0.00110	60.33	0.0	0
2	0.607	0.00050	59.73	-1.0	-6
3	0.616	0.00025	60.66	+0.5	+3
4	0.614	0.00070	60.38	+0.1	+1
5	0.610	0.00050	59.97	-0.6	-4

(a) Aerodynamic drag and required power for cases with opened splitline and yaw angle

Case #	$\dot{m}_{AC}$ $\left[\frac{kg}{sec}\right]$	$\dot{m}_{CAC}$ $\left[\frac{kg}{sec}\right]$	$\dot{m}_{radiator}$ $\left[\frac{kg}{sec}\right]$
1	0.885	3.258	2.937
2	0.472	0.916	0.763
3	1.202	1.645	1.452
4	0.000	0.000	0.000
5	1.138	1.557	1.448

(b) Mass flow of air through the cooling package for cases with opened splitline and yaw angle

Table 10: Closed splitline

Case #	C_d	C_d +/-	Power $[kW]$	% change of C_d vs ref. case	Drag counts vs ref. case
1	0.614	0.00075	60.42	0.2	+1
2	0.598	0.00065	58.86	-2.4	-15
3	0.610	0.00035	60.03	-0.5	-3
4	0.606	0.00020	59.67	-1.1	-7
5	0.607	0.00080	59.73	-1.0	-6

(a) Aerodynamic drag and required power for cases with closed splitline and yaw angle

Case #	$\dot{m}_{AC}$ $\left[\frac{kg}{sec}\right]$	$\dot{m}_{CAC}$ $\left[\frac{kg}{sec}\right]$	$\dot{m}_{radiator}$ $\left[\frac{kg}{sec}\right]$
1	0.674	3.043	2.727
2	0.006	-0.002	-0.032
3	0.993	1.1025	0.950
4	0.000	0.000	0.000
5	0.923	1.392	1.347

(b) Mass flow of air through the cooling package for cases with closed splitline and yaw angle

By analyzing the values in Table 9 and Table 10 it is seen that the C_d values are much higher than for the cases where the air is flowing with 0° yaw. Though, the magnitude of the C_d values can be considered as normal for the simulated conditions. The percentage change in C_d relative to the reference case is smaller than for the cases with 0° yaw.

For the cases with opened splitline the percentage change of the C_d values are both positive and negative, which is also different from the cases with no yaw, where all cases have a lower C_d than the reference case. Though, the variation of the C_d values for the opened splitline cases compared to the reference case with yaw, are never above 10 drag counts. For the closed splitline cases the largest difference in relation to the reference case is 15 drag counts and this result is obtained for Case 2. This case is the only case that has a drag counts reduction larger than 10 drag counts. The mass flow of air which passes the cooling system for the yaw angle cases is almost the same as for the cases with the air flowing with 0° yaw. This is seen when comparing the values in Table 5 and Table 7 with the values in Table 10b and Table 11b.

In Figure 24 the pressure distributions for the reference case having a yaw angle is viewed.

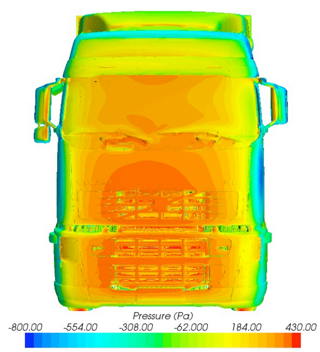

(a) Pressure distribution seen in a front view for the reference case

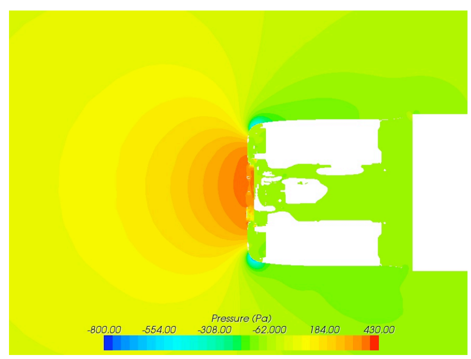

(b) Top view of the pressure distribution at the height z=1.5 m

Figure 24: Pressure distribution for the reference case with 5° yaw angle

By comparing these figures with the ones without any yaw, Figure 16 and Figure 17, it is easily seen that the stagnation area is no longer concentrated around the centerline of the vehicle. In Appendix C and D the pressure distribution figures for the cases with 5° yaw angle are presented. In Appendix F the velocity figures for the cases with 5° yaw are shown.

The isosurface when having the air flowing with 5° yaw does not have the same structure at all compared to the previous cases. In Figure 25 the isosurface front view for Case 1 with opened splitline is presented.

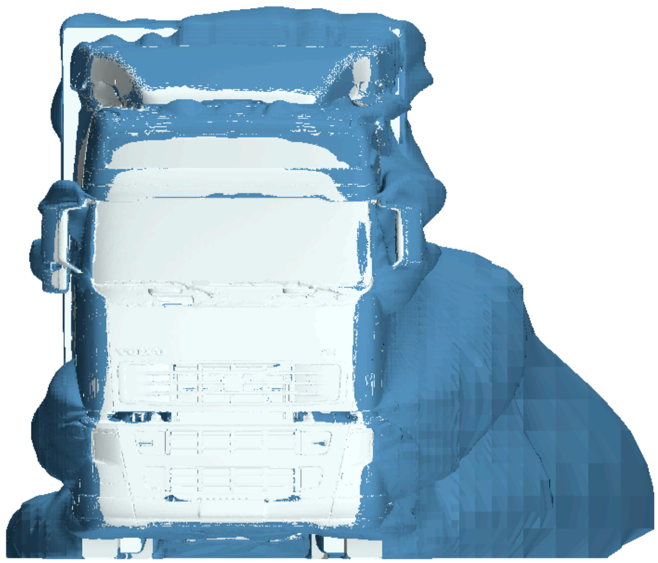

Figure 25: Isosurface for the reference case with yaw angle, Case 1 with opened splitline

The main difference between this figure and the figures of isosurface with no yaw is that for this case the leeward side of the vehicle has a larger area of isosurface compared to the other side. There is a large wake situated here since the air is flowing from the other side of the vehicle. There will be separation and turbulent areas in the wake and the air flow is no longer symmetric around the vehicle.

Table 11 represents the drag counts change between each opened and closed splitline case for the simulations run with 5° yaw.

Table 11: Drag counts change between each case with opened and closed splitline for 5° yaw

Case #	DC_{change}
1 closed - 1 opened	+1
2 closed - 2 opened	-9
3 closed - 3 opened	-6
4 closed - 4 opened	-7
5 closed - 5 opened	-3

The values in the table above show that, just as for the cases run with 0° yaw, Case 2 is most affected by a closed splitline.

6 Discussion

In this chapter the results from the simulations will be discussed. It should be noted that there are no exact solutions to the simulations, there are always sources of error. It should not be forgotten that the simulations are approximations of real-life conditions. From experience it is known that the error margin for the kind of simulations performed in this research is ± 10 drag counts and the results are discussed with this range in mind. Therefore, it may not be possible to discuss some of the results and draw any conclusions for these cases.

It is important for practical reasons, considering the technical solution intended to solve the variable cooling air intake area, to find a suitable combination of full and intermediate coverage of the cooling system. Hence, what should be determined is which of the grill or cooling package area that should be covered in order to lower the drag as much as possible.

When analyzing the cases with and without a covered splitline with 0° yaw, it is detected that all the geometrical changes that are made result in a reduction of aerodynamic drag compared to the reference case. This can be considered as a satisfying result since the aim with the different case set-ups is to lower the drag.

The results from the simulations that are run with 5° yaw angle show somewhat contradictive results. It is only Case 2 with closed splitline that shows results outside the error margin for the simulations. Therefore, the results from the 5° yaw simulations can not be used to the same extent as the 0° yaw angle cases.

From the velocity figures recirculating flow areas can be detected at the back side of the grill. This phenomenon is seen for all simulated cases where there is some kind of flow through the grill. The recirculation areas probably occur as a consequence of the sharp structure on the back side of the grill. These areas will most likely contribute to a higher aerodynamic drag. With a new, smoother design of the back side of the grill, these areas can be reduced or even be eliminated.

6.1 Opened versus closed splitline

A trend which is very clear to detect is that a covered grill in combination with a closed splitline generates lower drag compared to the remaining cases. Though, it should be said that the significance of the covered splitline differs between the different cases. For some cases the closed splitline reduces drag with 16 drag counts whereas for other cases the reduction is only a few drag counts, when comparing each corresponding opened and closed splitline case. But, the trend is still that a covered splitline is preferred for the cases with 0° yaw. The reduction in drag that is obtained for the closed splitline cases can be explained by an eliminated vortex structure in the splitline area, which is present for the opened splitline cases. These vortices can be seen in the figures of the isosurfaces shown in Chapter 5. Another explanation of the reduced aerodynamic resistance for the cases with closed splitline is that the mass flow of air through the cooling package is reduced, which may yield less surface friction and hence lower drag.

The cases that are most affected by the covered splitline are the cases where the grill is covered, i.e. Case 2 and Case 3. This can clearly be seen when comparing the reductions in drag for closed and opened splitline for these cases, shown in Table 8 on page 32. The same thing is also detected when analyzing the velocity figures for the corresponding cases; for the opened splitline cases it is clearly seen that the velocity is increased at the splitline area and indicates that more air is forced into the underhood area and thereby more drag is yielded. For the remaining cases, the difference in drag reduction between the opened and closed splitline cases lies within the error margin. However, the trend is still the same; a closed splitline reduces drag.

For all the cases with 5° yaw the influence of a closed splitline is neglectable since the difference in C_d values between the corresponding cases with opened and closed splitline are all within the error margin mentioned above. The C_d values are both increasing and decreasing for the different geometrical changes and hence no clear trend can be seen regarding the closed splitline. However, Case 2 is most influenced by the closed splitline. This result is obtained both for 0° yaw and 5° yaw. An explanation for this result is that the airflow through the cooling system is reduced with a closed splitline when comparing this value with the corresponding value for the opened splitline case.

For Case 2 with opened splitline and 0° yaw, drag is reduced by 17 drag counts compared to the reference case. Also, there is a significant mass flow of air through the cooling system which indicates that the cooling performance is quite adequate. Though, Case 2 with closed splitline results in a drag reduction of almost 33 drag counts compared to the reference case. Hence, the covered splitline contributes to the drag reduction by 16 drag counts. Case 2 is the case which has the largest difference in drag for closed versus opened splitline. Case 2 with closed splitline is also the case that has obtained the lowest aerodynamic drag values for all simulations. The reason for this is that the cooling airflow is completely eliminated, much due to the decreased surface friction between the air and the components in the underhood area, including the cooling system.

6.2 Grill versus cooling system

The technical solution that is intended to solve the variable cooling air intake area is desired to function both for full and intermediate coverage of the grill or cooling package. With this desire in mind together with the fact that a closed splitline is to be preferred, it can be concluded that covering the grill is more advantageous compared to covering the cooling package. This can be seen when comparing the results from the simulations; a covered grill for the closed splitline cases generates lower C_d values both for full and intermediate coverage of the cooling air intakes. Though, if no suitable technical solution for a covered grill area can be found, it is still worth to cover the cooling package and thereby reduce the aerodynamic drag. If this decision is made the results from these simulations show that the difference in savings of aerodynamic drag between full and intermediately coverage is negligibly small. Also, there is no motivation to make the decision to cover the splitline if it is desired to cover the cooling package. The possible savings in fuel consumption only due to a covered splitline for Case 4 and Case 5 are very small in relation to, for example, Case 2. The possible fuel consumption savings for Case 2 and Case 3 are 2.3% and 1.3%, respectively. The corresponding value for Case 4 and Case 5 is almost 1.2% for both cases.

Previous research made by Kuthada et al [6] shows that the higher amount of coverage of the grill results in lower aerodynamic drag. This is true for Case 2 with covered splitline since it has the lowest aerodynamic drag for Case 1-5. Though, this theory is not applicable for the remaining cases; there is no clear connection between the theory and the obtained results. The statement by Kuthada et al [6] is also true for Case 1, which has the largest airflow through the CAC and radiator. The cases with intermediately closed cooling system, i.e. Case 3 and Case 5, shows a higher amount of airflow through the AC condenser compared to the reference case. This can be explained by the fact that more air is forced through the grill or cooling component when the intake area is restricted.

6.3 Reflections

The trends of the results for the different methods of covering the cooling system can only be evaluated for the exact geometry- and case setup used in the simulations treated in this research. There have not been any wind tunnel tests to confirm the results from the simulations; it is fully possible that wind tunnel tests for the same vehicle configurations would have shown different results.

Comparing the cases with intermediate coverage, Case 3 and Case 5, it is seen that the results from the simulations are somewhat contradictive. For the simulations run with an opened splitline, it can be stated that it is better to cover the cooling package than the grill. Reversely, for the cases with closed splitline, it can be seen that it is preferable to cover the grill area. Though, it should be said that both of the results from the simulations with opened splitline lies within the error margin. Therefore, these results are not fully reliable. The simulations for Case 3 and Case 5 with closed splitline both show results that are outside the error margin. Hence, these results can be treated as more reliable than the results for opened splitline for Case 3 and Case 5. To be able to make any statements about Case 3 and Case 5 with opened splitline, further simulations must be run to find out if the same trends of the results are received.

For practically all simulations that are run where there is any mass flow of air through the cooling system, it is seen that the amount of air flowing through the radiator is less than flowing through the CAC. This means that there is some kind of leakage of air between these parts; ideally the airflow through these parts would have been identical since the size of the CAC and radiator is equal. There is a leakage protection shield mounted on the sides between the CAC and the radiator, but it can be shown from the results that it does not function properly. The reason why the air is leaking is that the resistance for the air flowing through the cooling system component is greater than the resistance for leaking around the protecting shield. The air also tends to flow through the CAC, but below the radiator. If these leakage problems could be solved, there would be less losses and the cooling system would work more efficiently.

The viscous dissipation factor will increase when air passes through the cooling system components, since these parts are constructed to increase the surface area around which the air flows. The larger the surface area for the air to stream around, the more resistance is produced. This fact can be used to explain the phenomenon of increased aerodynamic resistance when having opened cooling air intakes.

From the results it is seen that the largest drag reduction is obtained for Case 2 with closed splitline, the case where the cooling air intakes are fully covered. It is also seen when analyzing the figures of the pressure distribution for Case 2 with closed splitline compared to the reference case that the stagnation pressure area is reduced for Case 2. This can be seen as a somewhat unexpected result, since the front of the truck for Case 2 is entirely covered which from fundamental fluid dynamics would indicate that a larger stagnation area is created. The reason why the opposite result is obtained here can only be treated as speculations. A possible theory for this phenomenon is now described. When the entire grill area is closed, as in Case 2, the airflow in front of the vehicle is affected further away from the front than if the cooling air intakes are opened. This yields that the air is decelerated earlier, creating an air bubble in front of the cab. The air flowing towards the vehicle will be affected by the truck earlier and thereby a larger amount of the air will flow around the vehicle instead of flowing straight to the front and through the cooling system. A concept that perhaps would function like the air bubble in front of the vehicle is a so-called *soft nose*. This concept means that the front area of the truck is redesigned, to make the front more pointed and less blunt which helps to disturb the flow in front of the vehicle and guide the air better around the vehicle body. Another valuable function for the soft nose is that it acts like a deformation zone to protect occupants in crashes. Hence this solution has several valuable functions; the aerodynamics for the vehicle is most likely improved, and the safety for occupants in accidents is improved as well. However, an introduction of such a concept can lead to that the effect of a covered grill or cooling system is changed. In order to implement a soft nose, further CFD analysis is needed to confirm its function.

6.4 Discrepancy sources

Naturally, there are some discrepancy sources within this project. One source of error that can be mentioned is that the meshes are not exactly the same from case to case. Even though the total amount of cells is approximately the same, this method does not generate fully comparable solutions. Also, the amount of cells used in the models can be questioned. There may be a possibility that the results would have been different if the models were made with a higher resolution. Though, the amount of cells used for the models in this research can be considered as accurate comparing with other simulations made on similar models at Volvo 3P.

When running the simulations for the cases with 5° yaw angle the entire model is the same as for the cases with no yaw, except for the settings where the wind direction and rotational velocities of the wheels are set. Hence, the meshes are exactly the same as for the cases with no yaw. Due to this fact, the simulation results for the yaw cases may not be fully accurate. Since the air is flowing with a slight angle, the wake behind the vehicle will be displaced towards the side. Since the mesh is exactly the same as for the case with no yaw, the resolution of the wake for the yaw cases may be too low. This fact reduces the accuracy of the yaw cases. It would therefore be good to further resolve the mesh in the wake area for the yaw cases.

What could be interesting to investigate is to run the simulations with a different turbulence model. The model used, the $k\epsilon - model$, may not be fully suitable to resolve the wake behind the vehicle. For that purpose, it may have been better to use the $k\omega - model$. However, the $k\epsilon - model$ is a widely used turbulence model in the industry for the kinds of purposes treated here.

The truck and trailer model used for simulations in this research is a simplified model which does not completely correspond to a real Volvo FH16. For example, on the real truck there is a bug net mounted on the inside of the grill to prevent insects from fasten on the cooling package. There are also a large amount of cables and other smaller details that are not included in the model. Another factor is the trailer; there are various types of trailers available on the market, with different dimensions and features. The simulations performed here have only been using one type of trailer. If the simulations are done on a truck with all external and internal features that are present on a real truck and with another trailer attached to it, the simulation results would most likely be different. However, it should be said that overall the model used is rather complex and has a fairly detailed structure.

7 Conclusions and Recommendations

In this chapter the conclusions and recommendations for further work within the scope of this research are presented.

- All geometrical changes that are made to the reference model results in a decrease in C_d, for the cases where the values are outside the error margin.
- The most promising case that yields the most significant reduction in drag is Case 2 with closed splitline. This result is valid for all comparisons that are made, both for 0° yaw and 5° yaw.
- It is established that the concept with fully and intermediately covered grill, Case 2 and Case 3, is worth developing and should be further investigated. Case 2 with closed splitline and 0° yaw has a reduction of 33 drag counts compared to the reference case, which corresponds to a reduction in fuel consumption with 2.3%. Case 3 has a fuel consumption reduction of 1.3%.
- If no suitable technical solution can be found for covering the grill of the truck, it is still worth developing a device for covering the cooling package since there still is a quite substantial C_d reduction compared to the reference case. Both Case 4 and Case 5 with closed splitline show a reduction of 16 drag counts compared to the reference case, which corresponds to 1.2% reduction in fuel consumption.
- By re-designing the back side of the grill area, recirculation areas can be reduced or even eliminated. Thereby, there is a possibility to reduce the total aerodynamic drag.
- Case 2 with closed splitline has an air bubble in front of the vehicle which probably acts like a soft nose. A soft nose concept is recommended to further investigate in order to decrease the aerodynamic resistance for the truck.
- No adequate conclusions can be drawn from the cases simulated with 5° yaw, since all C_d reductions except for Case 2 with closed splitline lies within the error margin. One possible reason to these results is that the resolving of the wake structure is not adequate.
- It could be interesting to run the simulations with the $k\omega$ turbulence model instead to investigate the differences in resolving the wake structure for the different cases. It is recommended to resolve the mesh in the wake better in order to receive more accurate results from the cases simulated with 5° yaw.

References

[1] Air vent control - http://www.bmw.com, January 2009.

[2] Turbulence models - http://www.cfd-online.com/, May 2009.

[3] R H Barnard. *Road Vehicle Aerodynamic Design - An Introduction*. MechAero Publishing, 2001.

[4] Wei Ding, Jack Williams, and Dinakara Karanth. Cfd application in automotive front-end design. *SAE International*, (2006-01-0337), 2006.

[5] Hussein Jama, Simon Watkins, and Chris Dixon. Reduced drag and adequate cooling for passenger vehicles using variable area front air intakes. *SAE International*, (2006-01-0342), 2006.

[6] Timo Kuthada and Jochen Wiedemann. Investigations in a cooling air flow system under the influence of road simulation. *SAE International*, (2008-01-0796), 2008.

[7] David Söderblom. Investigation of wheel housing flow on heavy trucks. Technical report, 2009.

Appendix

A Pressure Distribution - Side View

B Pressure Distribution - Front View

C Pressure Distribution - Side View for 5° Yaw Angle

D Pressure Distribution - Front View for 5° Yaw Angle

E Velocity Distribution - Side View

F Velocity Distribution - Side View for 5° Yaw Angle

A Pressure Distribution - Side View

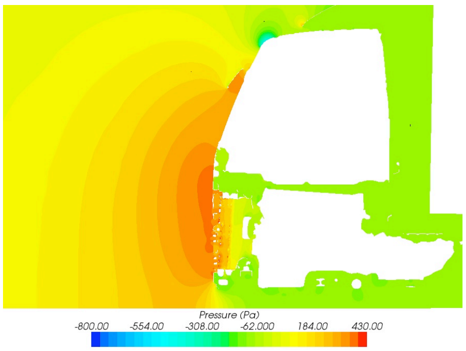

(a) Opened splitline

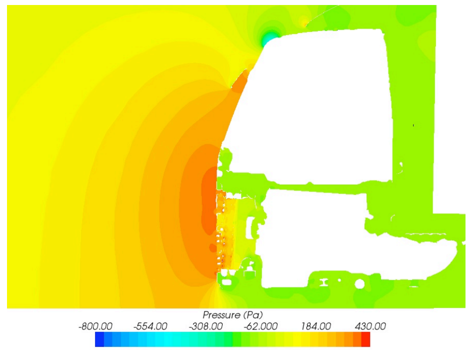

(b) Closed splitline

Figure A.1: Case1

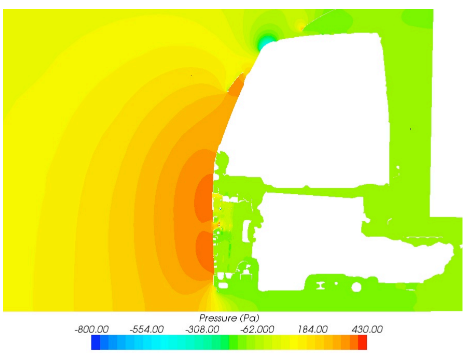

(a) Opened splitline

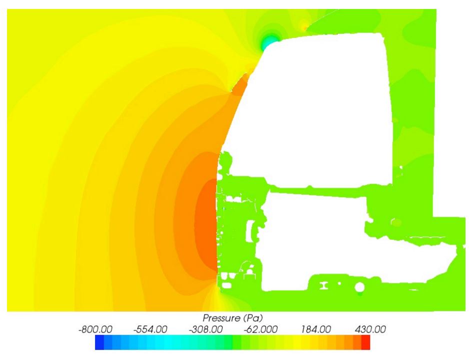

(b) Closed splitline

Figure A.2: Case 2

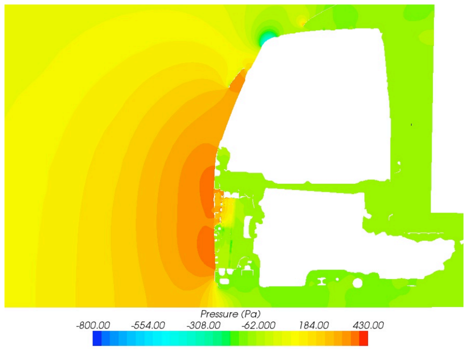

(a) Opened splitline

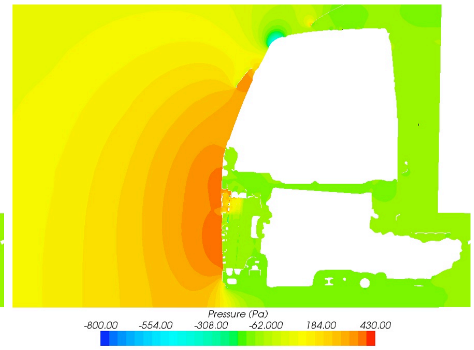

(b) Closed splitline

Figure A.3: Case 3

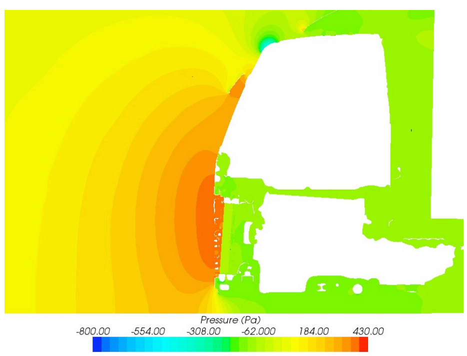

(a) Opened splitline

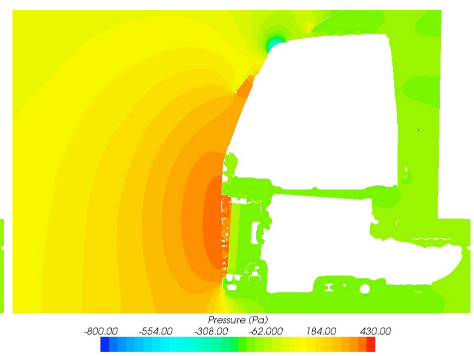

(b) Closed splitline

Figure A.4: Case 4

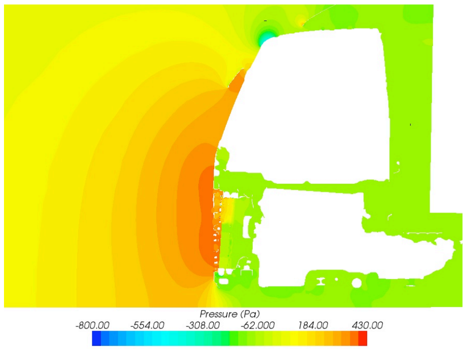

(a) Opened splitline

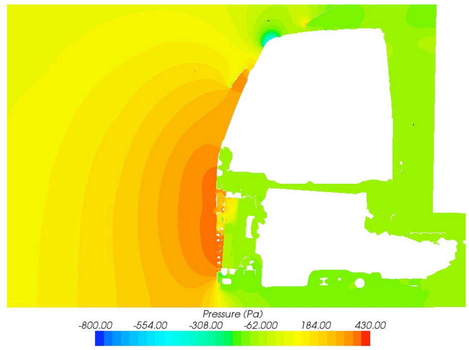

(b) Closed splitline

Figure A.5: Case 5

B Pressure Distribution - Front View

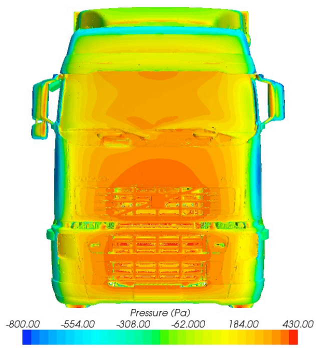

(a) Opened splitline

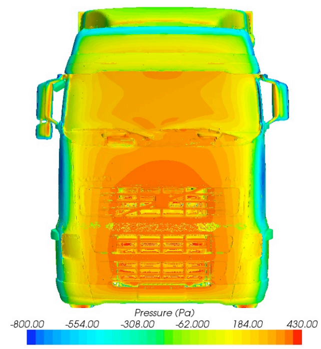

(b) Closed splitline

Figure B.1: Case1

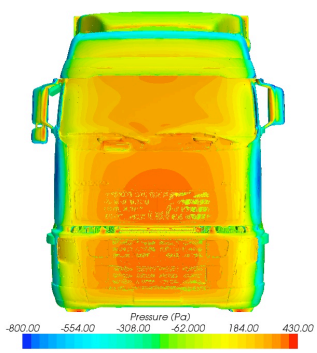

(a) Opened splitline

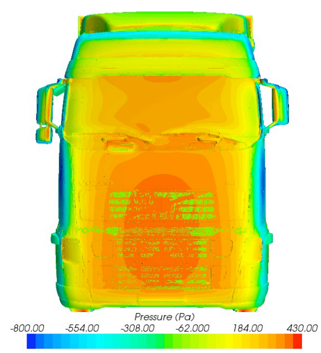

(b) Closed splitline

Figure B.2: Case 2

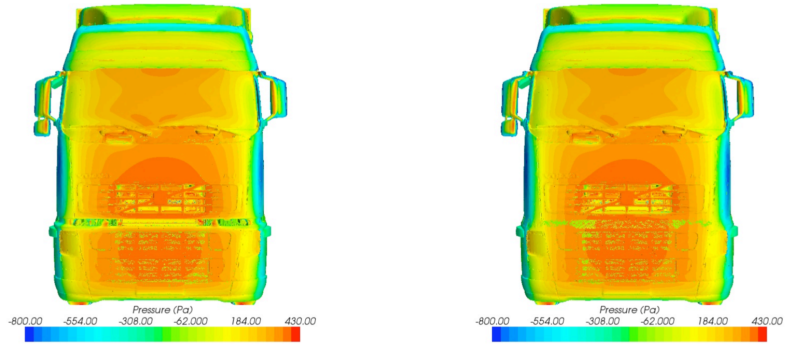

(a) Opened splitline (b) Closed splitline

Figure B.3: Case 3

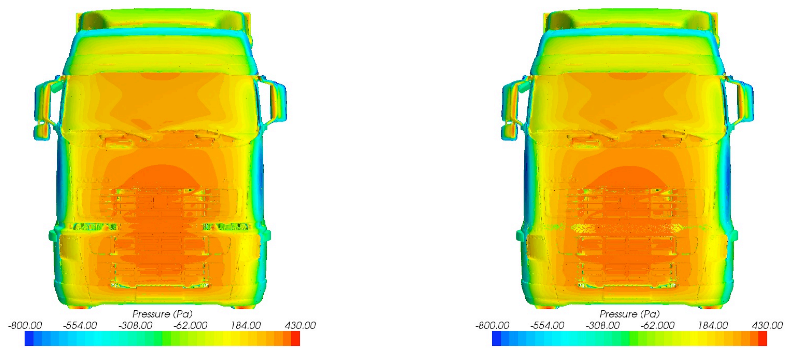

(a) Opened splitline (b) Closed splitline

Figure B.4: Case 4

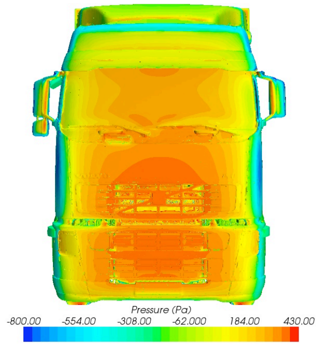

(a) Opened splitline

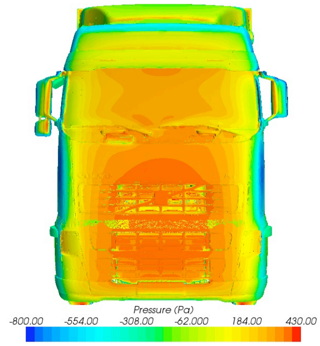

(b) Closed splitline

Figure B.5: Case 5

C Pressure Distribution - Side View for 5° Yaw Angle

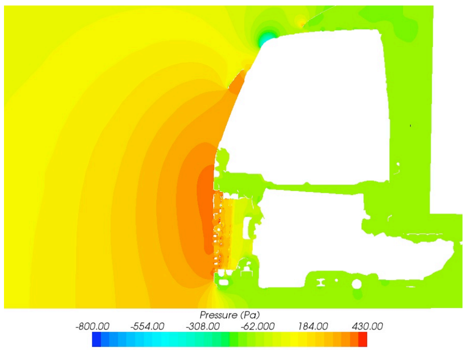

(a) Opened splitline

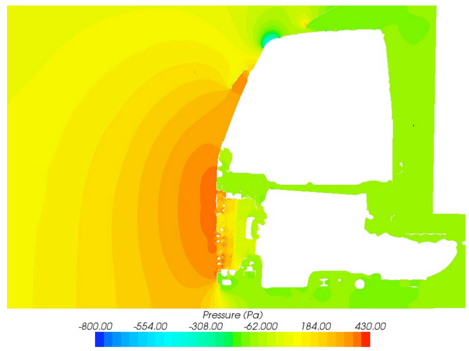

(b) Closed splitline

Figure C.1: Case1

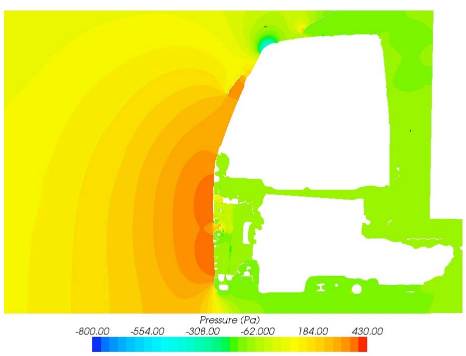

(a) Opened splitline

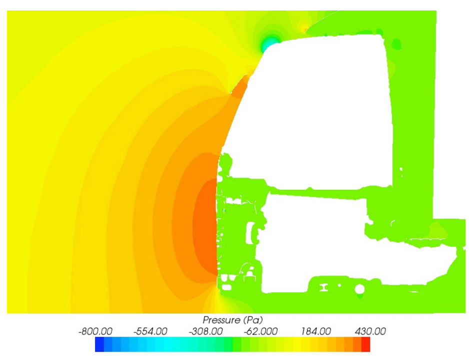

(b) Closed splitline

Figure C.2: Case 2

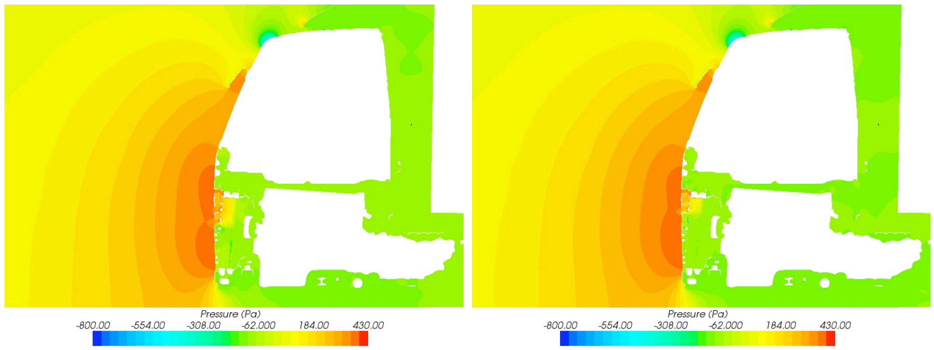

(a) Opened splitline (b) Closed splitline

Figure C.3: Case 3

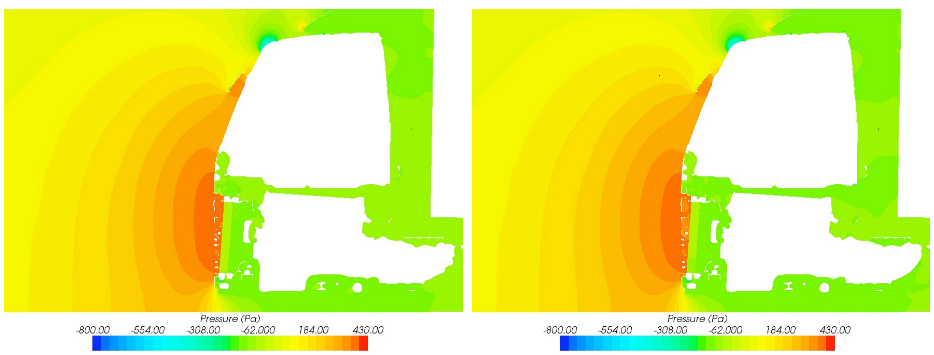

(a) Opened splitline (b) Closed splitline

Figure C.4: Case 4

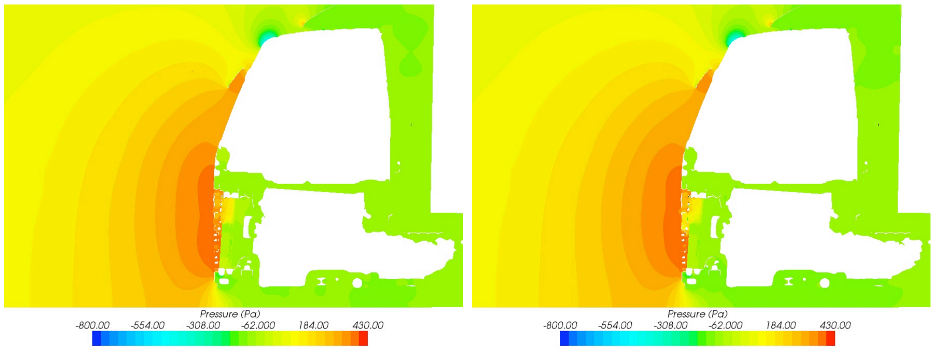

(a) Opened splitline (b) Closed splitline

Figure C.5: Case 5

D Pressure Distribution - Front View for 5° Yaw Angle

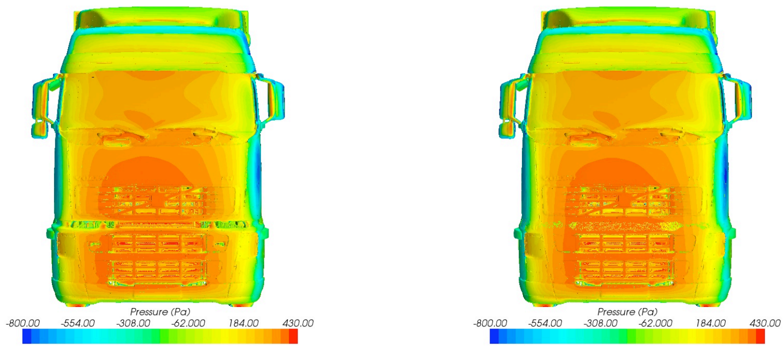

(a) Opened splitline (b) Closed splitline

Figure D.1: Case1

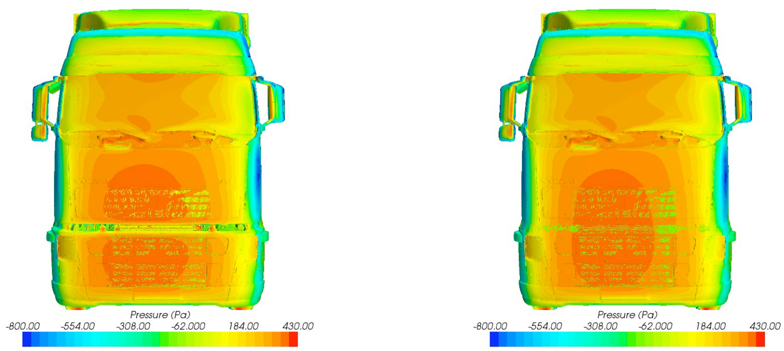

(a) Opened splitline (b) Closed splitline

Figure D.2: Case 2

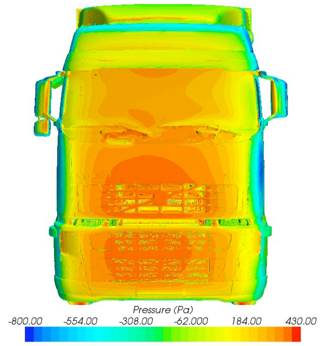

(a) Opened splitline

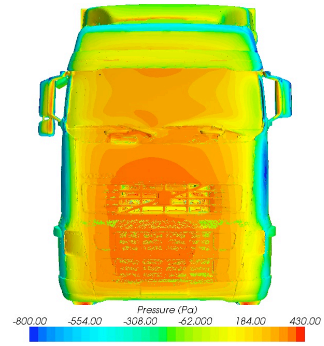

(b) Closed splitline

Figure D.3: Case 3

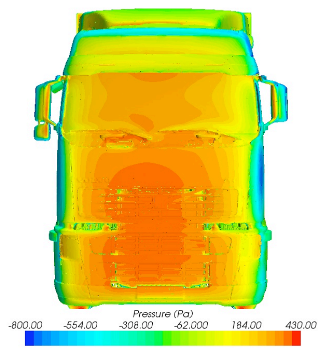

(a) Opened splitline

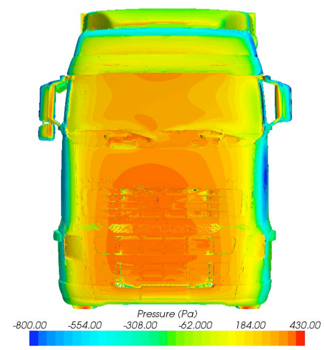

(b) Closed splitline

Figure D.4: Case 4

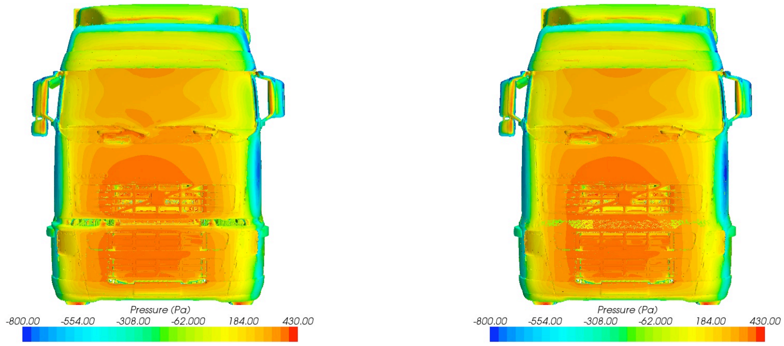

(a) Opened splitline (b) Closed splitline

Figure D.5: Case 5

E Velocity Distribution - Side View

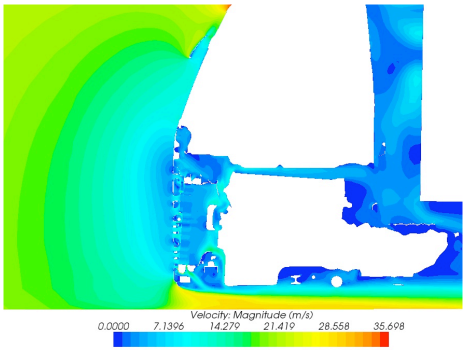

(a) Opened splitline

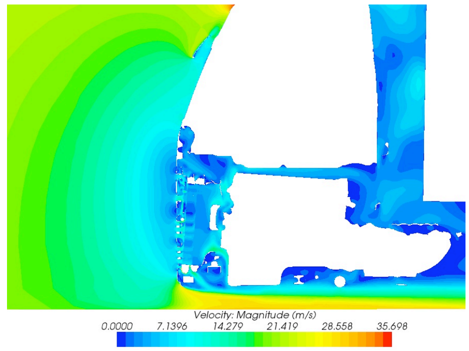

(b) Closed splitline

Figure E.1: Case1

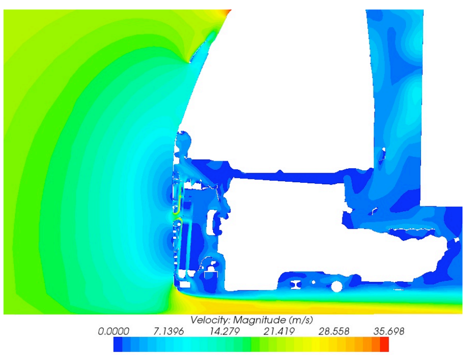

(a) Opened splitline

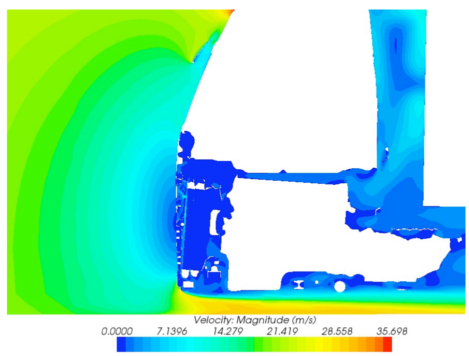

(b) Closed splitline

Figure E.2: Case 2

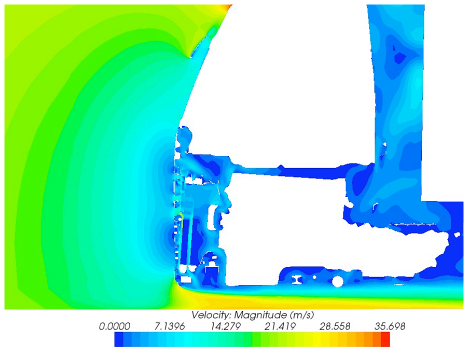

(a) Opened splitline

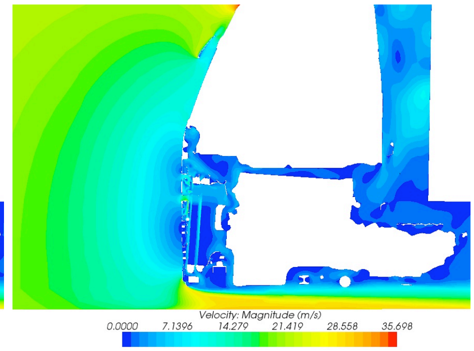

(b) Closed splitline

Figure E.3: Case 3

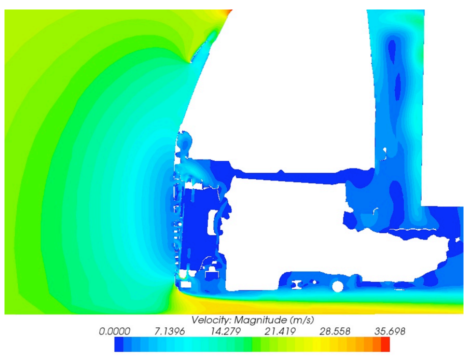

(a) Opened splitline

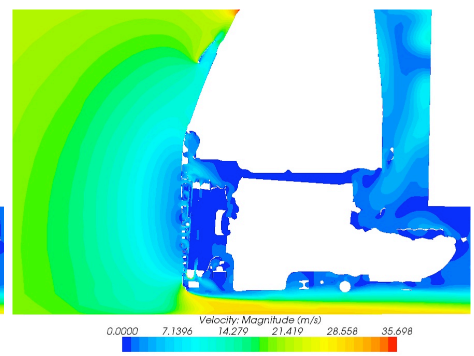

(b) Closed splitline

Figure E.4: Case 4

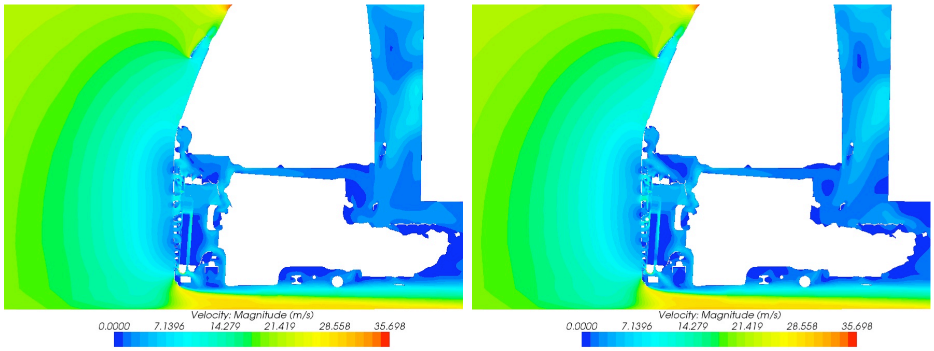

(a) Opened splitline (b) Closed splitline

Figure E.5: Case 5

F Velocity Distribution - Side View for 5° Yaw Angle

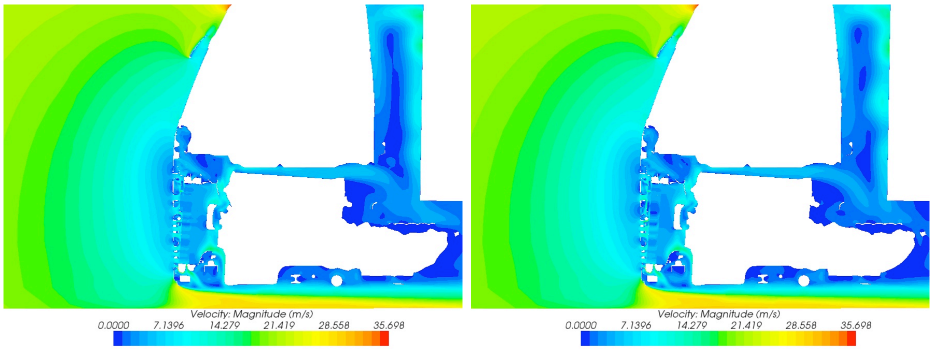

(a) Opened splitline (b) Closed splitline

Figure F.1: Case1

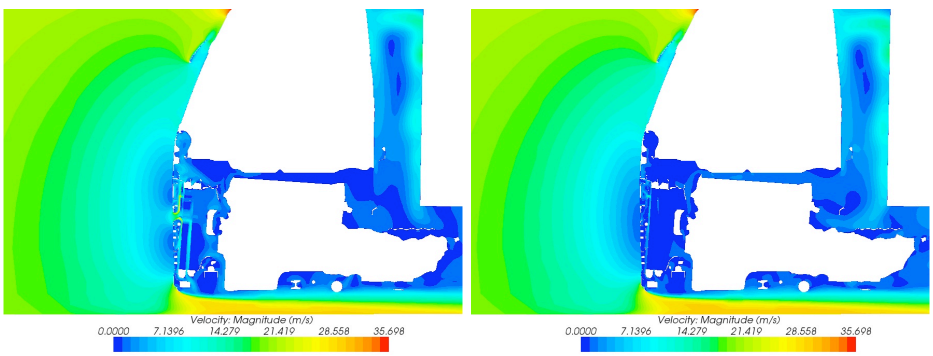

(a) Opened splitline (b) Closed splitline

Figure F.2: Case 2

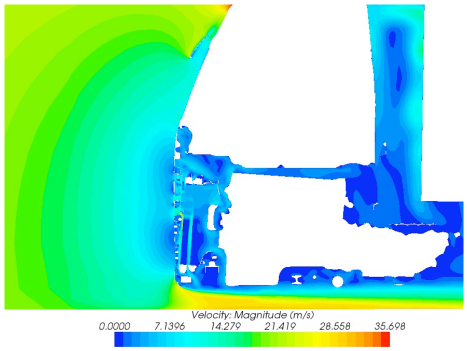

(a) Opened splitline

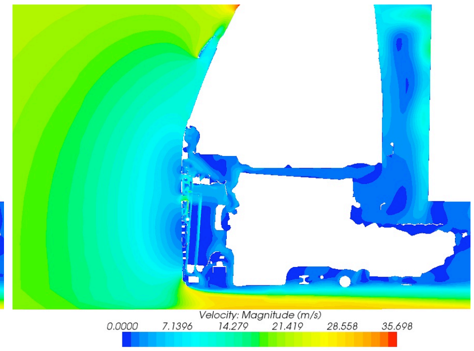

(b) Closed splitline

Figure F.3: Case 3

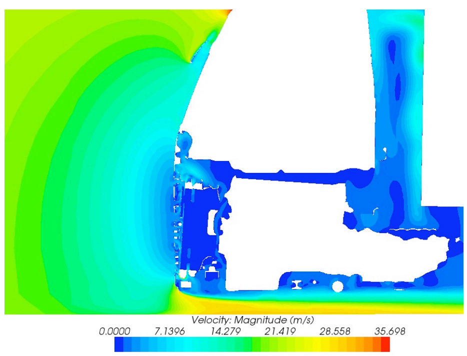

(a) Opened splitline

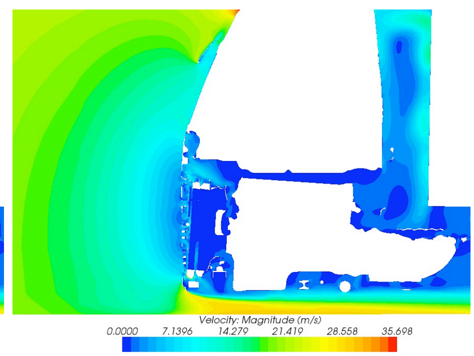

(b) Closed splitline

Figure F.4: Case 4

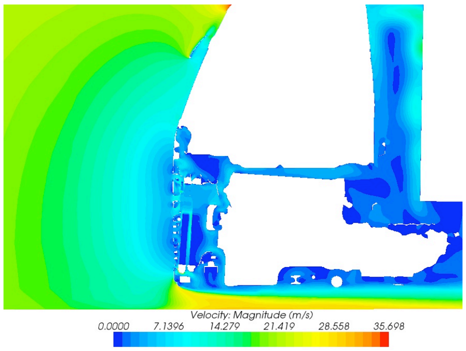

(a) Opened splitline

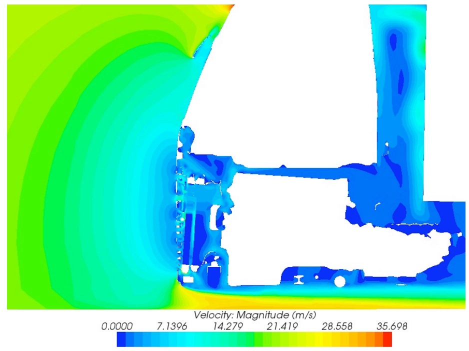

(b) Closed splitline

Figure F.5: Case 5